Published in final edited form as:
Cell Microbiol. 2008 June ; 10(6): 1286–1303. doi:10.1111/j.1462-5822.2008.01126.x.

The Δ*fbpA* mutant derived from *Mycobacterium tuberculosis H37Rv* has an enhanced susceptibility to intracellular antimicrobial oxidative mechanisms, undergoes limited phagosome maturation and activates macrophages and dendritic cells

Muralidhar K. Katti[1,†], **Guixiang Dai**[1,†], **Lisa Y. Armitige**[1], **Carlos Rivera Marrero**[2], **Sundarsingh Daniel**[1], **Christopher R. Singh**[1], **Devin R. Lindsey**[1], **Subramanian Dhandayuthapani**[3], **Robert L. Hunter**[1], and **Chinnaswamy Jagannath**[1,*]

[1]Department of Pathology and Laboratory Medicine, University of Texas Health Sciences Center, Houston, TX, USA.

[2]Department of Pulmonary Medicine, School of Medicine, Emory University, Atlanta, GA, USA.

[3]Regional Academic Health Center, UTHSC, Edinburg TX, USA.

Summary

Mycobacterium tuberculosis H37Rv (Mtb) excludes phagocyte oxidase (*phox*) and inducible nitric oxide synthase (iNOS) while preventing lysosomal fusion in macrophages (MΦs). The antigen 85A deficient (Δ*fbpA*) mutant of Mtb was vaccinogenic in mice and the mechanisms of attenuation were compared with MΦs infected with H37Rv and BCG. Δ*fbpA* contained reduced amounts of trehalose 6, 6, dimycolate and induced minimal levels of SOCS-1 in MΦs. Blockade of oxidants enhanced the growth of Δ*fbpA* in MΦs that correlated with increased colocalization with *phox* and iNOS. Green fluorescent protein-expressing strains within MΦs or purified phagosomes were analysed for endosomal traffick with immunofluorescence and Western blot. Δ*fbpA* phagosomes were enriched for *rab*5, *rab*11, LAMP-1 and Hck suggesting enhanced fusion with early, recycling and late endosomes in MΦs compared with BCG or H37Rv. Δ*fbpA* phagosomes were thus more mature than H37Rv or BCG although, they failed to acquire *rab7* and CD63 preventing lysosomal fusion. Finally, Δ*fbpA* infected MΦs and dendritic cells (DCs) showed an enhanced MHC-II and CD1d expression and primed immune T cells to release more IFN-γ compared with those infected with BCG and H37Rv. Δ*fbpA* was thus more immunogenic in MΦs and DCs because of an enhanced susceptibility to oxidants and increased maturation.

Introduction

Tuberculosis is the leading cause of mortality owing to infections in man today with at least 3 million deaths reported worldwide (Harries and Dye, 2006). The causative agent *Mycobacterium tuberculosis* (Mtb) has the unique ability to survive within macrophages (MΦs) using diverse strategies and become dormant, but reactivate to cause adult tuberculosis. The ability of Mtb to survive within the hostile environment of MΦs depends upon several unique features. The MΦs generate reactive oxygen species (ROS) from

*For correspondence. chinnaswamy.jagannath@uth.tmc.edu; Tel. (+1) 713 500 5353; Fax (+1) 713 500 0730..
†These authors contributed equally to the manuscript.

NADPH oxidase (phagocyte oxidase; *phox*) and nitric oxide (NO) via inducible nitric oxide synthase (iNOS) to kill intracellular pathogens. The phagosome–lysosome (P-L) fusion followed by enzymatic degradation appears to be another major mechanism of pathogen destruction (Nathan, 1983; Clemens, 1996; Deretic *et al.*, 1997; Russell, 2001). Earlier studies have shown that virulent strains of Mtb and BCG strains produce abundant superoxide dismutase that inactivates superoxide, shed abundant lipids that scavenge ROS and modulate ROS in human neutrophils (Scherer *et al.*, 1997; Perskvist *et al.*, 2002a). Interestingly, H37Rv and BCG phagosomes also prevent colocalization of iNOS and *phox* with their phagosomes within MΦs (Scherer *et al.*, 1997; Perskvist *et al.*, 2002a; Miller *et al.*, 2004; Daniel *et al.*, 2006). Armstrong and Hart (1971) made the seminal observation that Mtb phagosomes do not fuse with lysosomes in MΦs that eventually led to the unraveling of a unique mechanism of pathogen survival. Thus, it seems clear that Mtb has multiple strategies to bypass MΦ antimicrobial mechanisms and become a successful pathogen.

A vaccine has been proposed to be the most effective means to prevent tuberculosis (Donald *et al.*, 2007). However, the mechanisms through which successful vaccines can be developed remain complex. The widely used BCG vaccine has a variable efficacy (0–80%) in children, geographic variability and does not protect against adult tuberculosis (Fine, 1989; Brewer and Colditz, 1995; Fine, 2001). As a consequence, several attenuated strains of Mtb have been produced and tested in animal models as potential vaccines. The isocitrate lyase (*icl*) knockout (KO) mutant of Mtb had reduced virulence compared with the wild type in mice, but the organisms were still present in sufficient numbers in the organs to preclude vaccination strategies (McKinney *et al.*, 2000). The mammalian cell entry (*mce*) gene mutant was attenuated but was virulent through specific routes in mice (Gioffre *et al.*, 2005). We first reported that an attenuated mutant of H37Rv which lacked the expression of antigen 85A (Δ*fbpA*) offered better protection than BCG against tuberculosis in the mouse model (Copenhaver *et al.*, 2004). Subsequently, a pantothenate auxotroph of Mtb was found attenuated in mice and also protect mice against a lethal challenge with virulent Mtb, but the protection afforded was inferior to that provided under similar circumstances with BCG (Sambandamurthy *et al.*, 2002). More recent reports show that double gene KO strains from Mtb offer better protection than BCG in mice and safer in immunodeficient mice (Sambandamurthy *et al.*, 2006). These studies lend an optimism that attenuated candidate vaccines can be derived from pathogenic Mtb, although, the molecular basis and rationale for the use of Mtb-derived vaccines remains confusing because of the perplexing relationships between attenuation and immunogenicity.

It is generally held that, for bacterial strains to be effective vaccines, they need to be killed and processed efficiently by antigen-presenting cells (APCs) like MΦs and dendritic cells (DCs) (Harding, 1991). This involves oxidative killing followed by lysosomal destruction, where enzymes degrade microbial proteins into peptides that are then exported to the MHC-II containing compartments (MIIC) and presented in the context of MHC-II to CD+ T cells (Harding, 1991; Levine and Chain, 1991). There is of course, a cytosol dependent processing of antigens for MHC-I presentation (Harding, 1991). Paradoxically, these mechanisms appear deficient during antigen presentation by mycobacterial vaccines. For example, virulent Mtb as well as BCG prevent P-L fusion in MΦs (Clemens, 1996; Russell, 1998; Deretic and Fratti, 1999). Mtb has been found to downregulate the expression of MHC-II in MΦs and desensitize them for the activating effects of IFN-γ (Noss *et al.*, 2000) (Banaiee *et al.*, 2006). Human monocytes and mouse MΦ infected with Mtb show defective antigen presentation (Pancholi *et al.*, 1993; Gercken *et al.*, 1994; Ramachandra *et al.*, 2001). Modulation of MΦ function by Mtb has been shown to correlate with certain immunosuppressive antigens (Stewart *et al.*, 2005). We recently showed that attenuated BCG and wild-type H37Rv do not efficiently present certain immunodominant antigens like antigen 85B to T cells, an event related to phagosome maturation arrest (Singh *et al.*, 2006).

Together, these studies suggest that wild-type Mtb and to a certain extent BCG vaccine appear to modulate the ability of MΦs to be immunogenic for T cells. This raised a question whether attenuated Mtb-derived candidate vaccines similarly affect MΦs. Therefore, in this study, we have compared the intracellular survival strategies of a novel Δ*fbpA* mutant derived from H37Rv with the BCG vaccine and wild-type H37Rv. We have analysed the differences in cell wall lipids and modulation of signal transduction and correlated them to intracellular susceptibility for oxidants, endosomal traffic and activation of APCs. We demonstrate that Δ*fbpA* is deficient in cell wall lipids and more susceptible to the antibacterial mechanisms of MΦs. We suggest that the immunogenicity of mycobacterial vaccines may well depend upon an efficient intracellular processing by APCs.

Results

Deletion of fbpA alters the phenotype with alterations in cell wall lipids

That *fbpA, fbpB* and *fbpC* transfer mycolic acids to trehalose to synthesize 6,6, trehalose dimycolate (TDM) is well established (Belisle *et al.*, 1997). Our gene disruption studies indicated that Δ*fbpA* and Δ*fbpB* had different phenotypes, Δ*fbpA* being attenuated and Δ*fbpB* remaining unchanged (Armitige *et al.*, 2000; Copenhaver *et al.*, 2004). In order to determine whether deletion of *fbpA* affected lipids, we analysed the mycolic acid content of whole cells using column purification of followed by thin layer chromatography (TLC). Initial studies showed no differences in the content of alpha, keto and methoxymycolic acids between the three strains during TLC analysis (not shown). We then determined the cell wall content of TDM using radioisotope incorporation into the wild-type H37Rv, Δ*fbpA* and the reconstituted Δ*fbpA*. The strains were cultured in broth and metabolically labelled with ^{14}C-acetate and incorporation into TDM measured using TLC analysis of cell wall extracts followed by spectroscopy. Figure 1 shows that Δ*fbpA* had a decreased incorporation of the label into cell wall derived from TDM compared with H37Rv while the reconstituted mutant incorporated levels more than the wild type. We suggest that overexpression of *fbpA* gene in the multiple copy plasmids may have enhanced ^{14}C-acetate incorporation.

*Δ*fbpA modulates signal transduction in MΦs through the reduced expression of suppressor of cytokine signalling 1

BCG and Mtb as well as their product TDM strongly induce suppressor of cytokine signalling 1 (SOCS-1) in MΦs (Imai *et al.*, 2003). SOCS-1 in turn, has been found to desensitize MΦ response to IFN-γ, affect maturation of dendritic cells (DCs) and suppress the MHC-II expression of DCs and MΦs in response to IFN-γ (O'Keefe *et al.*, 2001; Bartz *et al.*, 2006). We hypothesized that the differences in the cell wall content of TDM in mycobacteria may affect their ability to induce SOCS-1 and thereby, the ability to modulate MΦs and DCs. MΦs were infected with Δ*fbpA*, BCG and H37Rv followed by analysis of SOCS-1 levels by Western blot. MΦs showed an early and strong expression of SOCS-1 when infected with either BCG or H37Rv that continued over 4 h (Fig. 2A). In contrast, Δ*fbpA* induced none at 1 h post infection, while, trace levels of SOCS-1 were apparent in MΦs by 4 h. The positive control TDM by itself induced a strong signal for SOCS-1 (Fig. 2B). A nearly identical profile was found also in immature DCs purified from bone marrows of mice (not shown). As SOCS-1 desensitizes MΦs to the effects of IFN-γ, we tested the susceptibility of Δ*fbpA*, BCG and H37Rv infected MΦs to 400 U ml^{-1} of IFN-γ followed by colony-forming unit (cfu) counts 48 h later. Figure 2C illustrates that under these conditions, IFN-γ activated MΦs were able to kill Δ*fbpA* better than BCG or H37RV, killing more 0.8 $\log_{10}$ organisms in 48 h. These results suggest that Δ*fbpA* was more susceptible to the bactericidal mechanisms induced by IFN-γ in MΦs compared with BCG or H37Rv.

*Growth curves of Δ*fbpA, BCG and wild-type H37Rv in murine MΦs and susceptibility to oxidants

We have previously described the growth profiles of Δ*fbpA* mutant and wild-type H37Rv in the murine J774.A1 and human THP1 MΦs (Copenhaver *et al.*, 2004). Figure 3A shows that the mutant had a similar inability to grow in un-activated primary murine MΦs, while, H37Rv registered a significant growth. BCG was also attenuated. Prior activation of MΦs with IFN-γ reduced the cfu counts of all three strains well below that found for the same strains in naïve MΦs. This is consistent with the known ability of IFN-γ to preactivate MΦs and the reduced response of mycobacteria infected MΦs to the activation effects of IFN-γ (Gercken *et al.*, 1994; Banaiee *et al.*, 2006). As IFN-γ activates oxidant response in MΦs, intracellular susceptibility of mycobacteria to oxidants, was determined by incubating infected MΦs with diphenylene iodonium (DPI), a ROS inhibitor and NG-monomethyl-l-arginine (NMMA), an inhibitor of NO synthesis or their combination. Preliminary studies showed that among inhibitor-treated MΦs, between days 5–7, excessive growth of wild-type Mtb detached MΦs after infection. Thus, in order to maintain the integrity of MΦs and avoid errors in bacterial counts, cfu were determined on day 3 post treatment. Figure 3B shows that both DPI or NMMA enhanced the growth of Δ*fbpA,* although their combination was more effective. In contrast, the growth of H37Rv was significantly enhanced only with NMMA but not DPI. BCG showed a modest increase in growth when NO was blocked through NMMA. These results suggest that Δ*fbpA* was susceptible to the individual and combined action of ROS and NO within MΦs. The wild type and BCG were more susceptible to intracellular NO and less susceptible to ROS.

Increased intracellular targeting of phox and iNOS to ΔfbpA *phagosomes in MΦs*

NO is produced by iNOS that assembles against the phagosomal membrane, and ROS is produced by the *phox* enzyme that also colocalizes against bacterial phagosomes in MΦs (Vazquez-Torres and Fang, 2001; Miller *et al.*, 2004; Daniel *et al.*, 2006). In order to determine whether susceptibility to oxidants (Fig. 3B) correlated with the increased intracellular targeting of iNOS and *phox*, MΦs were infected with *gfp* Δ*fbpA, gfpH* 37Rv or *gfp*BCG and immunostained for iNOS and $p47^{phox}$ proteins. MΦs were stained untreated and after IFN-γ activation. Colocalization was determined using laser confocal scanning microscopy (LSM). Figure 4A illustrates that *gfp* Δ*fbpA* had an increased targeting with iNOS using a specific mab compared with *gfpH* 37Rv or *gfp*BCG phagosomes in naïve MΦs. The quantitative scoring of colocalizations derived from triplicate experiments using naïve MΦs is shown below that confirms an enhanced targeting of iNOS to *gfp* Δ*fbpA* phagosomes (Fig. 4B). A similar profile was observed for colocalization of these strains with $p47^{phox}$; *gfp* Δ*fbpA* acquired more *phox* than either *gfpH* 37Rv or *gfp*BCG (Fig. 4C and D). As a positive control, MΦs were activated with IFN-γ that markedly increased the colocalization of *phox* and iNOS to *gfp* Δ*fbpA, gfp*BCG and *gfpH* 37Rv phagosomes. As more than 75% of phagosomes of these three strains acquired *phox* and iNOS, and no significant differences in colocalization were found after IFN-γ activation, data are not shown separately. However, these positive control studies confirmed that the bactericidal mechanisms of MΦs were intact and activated by IFN-γ.

*Increased oxidant activity in MΦs infected with Δ*fbpA

As a combination of DPI and NMMA increased the growth of Δ*fbpA* (Fig. 3B), and oxidant-producing enzymes colocalized with Δ*fbpA* phagosomes within MΦs (Fig. 4), additional studies were performed to confirm the levels of intracellular ROS as well as NO released by the infected MΦs. The intracellular ROS measured using dihydrodichloro-fluorescein diacetate (H_2DCFDA) was expressed as mean fluorescence intensity (MFI) using flow cytometry. Δ*fbpA* induced higher and sustained levels of ROS than either H37Rv or BCG in MΦs (Fig. 5A). In additional studies, quantitative techniques were used

to measure and compare the intracellular accumulation of oxidants; ROS was measured using fluorometry and NO by colorimetry. Δ*fbpA* infected MΦs again contained higher levels of ROS as well as the NO-derived product, nitrite (Fig. 5B and C). Data indicate that decreased growth of Δ*fbpA* in MΦs was likely due to an increased oxidative activity.

Enhanced acquisition of early and late endosomal markers by Δ fbpA *phagosomes*

Endosome fusion events precede P-L fusion which is the third mechanism that is known to kill intracellular bacteria and we sought to determine if Δ*fbpA* was attenuated because of increased P-L fusion (Clemens, 1996; Russell, 1998; Vieira *et al.*, 2002; Vergne *et al.*, 2004a). Virulent Mtb phagosomes are known to fuse selectively with early endosomes while excluding late endosomes as well as lysosomes (Clemens and Horwitz, 1996; Deretic *et al.*, 1997; Russell, 2001). The early endosomes deliver nutrients and organelles to enable growth of bacteria. In order to determine the sequential endosome fusion events, MΦs were first loaded with endocytic tracers, chased and infected with *gfp*-mycobacteria for 4 h. Colocalization was determined using LSM. Figure 6A illustrates that *gfp* Δ*fbpA* rapidly colocalized with the acidotropic dye LTR, while *gfpH* 37Rv excluded LTR. The ability of H37Rv to exclude LTR is consistent with similar previous reports (Via *et al.*, 1997). LSM studies were also performed using the early endosome marker, transferrin Texas red (TRR) and the late endosomal marker, mannosylated BSA rhodamine (MBR). The time bound colocalization of LTR, MBR and TRR by mycobacterial phagosomes within MΦs is shown in Fig. 6B. All three mycobacterial phagosomes were similar in the acquisition of TRR, an early endosomal marker. However, *gfp* Δ*fbpA* phagosomes showed an enhanced capacity to fuse with late endosomes (LTR and MBR) when compared with either *gfpH* 37Rv or *gfp*BCG.

*Phagosomes of Δ*fbpA acquire phagosome maturation markers but exclude lysosomal markers

Mycobacteria growing within MΦs fuse differentially with early and late endosomes depending upon their virulence, but virulent strains such as H37Rv do not fuse with lysosomes (Via *et al.*, 1998; Fratti *et al.*, 2000). As P-L fusion leads to mycobacterial killing, we sought to determine if Δ*fbpA* was attenuated because of an altered ability to fuse with lysosomes. In order to characterize this event, two types of markers were analysed. Lysosomes of murine and human MΦs express CD63 and *rab*7 markers (Clemens and Horwitz, 1995; Astarie-Dequeker *et al.*, 1999; Astarie-Dequeker *et al.*, 2002; Fratti *et al.*, 2003). Other lysosomal markers such as lysosome-associated membrane protein 1 (LAMP-1) and the *src* family kinase, Hck have been reported to occur also on late endosomes (Mommaas *et al.*, 1995; Astarie-Dequeker *et al.*, 2002; Perskvist *et al.*, 2002b). For example, LAMP-1 is present on all mycobacterial phagosomes but at variable levels on virulent and avirulent strains (Ullrich *et al.*, 1999; Fol *et al.*, 2006). MΦs infected with *gfp*-expressing mycobacteria were separately labelled with fluorescent tagged antibodies to LAMP-1, Hck, CD63 and *rab*7 in an effort to colocalize the mycobacteria with these markers. Figure 7A and 7B illustrates that *gfp*Δ*fbpA* phagosomes colocalized with Hck but not with *rab*7. Quantitative scoring of colocalization indicated that the mutant phagosomes stained for LAMP-1 and Hck more than BCG vaccine or H37Rv but excluded the lysosome-specific markers, CD63 and *rab*7 (Fig. 7C).

In additional confirmatory studies, MΦs were infected with mycobacterial strains and latex bead controls followed by sucrose gradient purification of phagosomes. The latter were analysed using Western blot with a panel of antibodies directed against early endosomes (*rab*5A, *rab*5B), recycling endosomes (*rab*11), late endosomes (LAMP-1, Hck) and lysosomes (CD63, *rab*7). An antibody against phosphatidyl inositol 3-kinase (PI-3K) was also used, as it has been reported to be one main regulator of endosomal docking process

(Deretic *et al.*, 1997; Deretic and Fratti, 1999; Deretic *et al.*, 2004). Western analysis showed interesting results (Fig. 7D). As anticipated, the latex beads that are known to undergo rapid P-L fusion expressed multiple markers of lysosomal fusion including CD63 and *rab7*. Δ*fbpA* phagosomes were enriched for the docking proteins, *ra5A* and rab*5B* that characterize early endosomes while they excluded *rab7*, the marker of lysosomes as well as CD63, another marker of lysosomes (Fig. 7D). They were also enriched for *rab11*, a marker for recycling endosomes and for PI-3K. In addition, Δ*fbpA* phagosomes readily acquired the late endosomal markers such as Hck and LAMP-1 when compared with either H37Rv or BCG. The latter excluded CD63, *rab7* and *rab11* consistent with their previously reported behaviour (Deretic *et al.*, 1997; Deretic and Fratti, 1999; Deretic *et al.*, 2004). Previous studies show that wild-type H37Rv acquires the early endosomal marker *rab5* but excludes the lysosomal marker *rab7* in MΦs, and are thus known to be 'immature' phagosomes and 'arrested' at the level of early endosomes (Via *et al.*, 1997; Russell, 2001). As Δ*fbpA* phagosomes acquired *rab5, rab11* and PI-3K, we suggest that their phagosomes were more mature than either H37Rv or BCG phagosomes in MΦs, but were still not competent to fuse with the lysosomes.

*MΦs and dendritic cells (DCs) infected with Δ*fbpA *have a more mature phenotype*

Virulent H37Rv strain of Mtb downregulates the expression of MHC-II in MΦs as well as desensitizes the MΦs to the activating effects of IFN-γ (Noss *et al.*, 2000; Banaiee *et al.*, 2006). BCG has also been shown to subvert the phenotype of APCs like DCs affecting their maturation status (Gagliardi *et al.*, 2005). Furthermore, both Mtb and BCG induce SOCS-1 in MΦs that can inhibit the activating effects of IFN-γ (Imai *et al.*, 2003; Manca *et al.*, 2005). To investigate whether Δ*fbpA* influenced the phenotype of APCs, MΦs and DCs were first infected with Δ*fbpA,* H37Rv and BCG and then tested for the surface expression of receptors using immunocytometry. Figure 8A illustrates the histograms of infected MΦs while, the footnote Table outlines the MFI values obtained from three independent experiments. MΦs infected with Δ*fbpA* had an enhanced expression of MHC-II, CD1d, CD86 and CD40 when compared with MΦs infected with either H37Rv or BCG. CD80 expression was comparable. Similarly, among DCs, Δ*fbpA* enhanced the expression of MHC-II, CD1d and CD40 but not CD80 or CD86 (Fig. 8B). These studies suggested that Δ*fbpA* infected MΦs and DCs have a more activated phenotype than those infected with either BCG or H37Rv.

Antigen presentation by APCs infected with mycobacteria

Phagosome maturation and fusion with lysosomes has been suggested to be a prelude to microbial degradation, loading of peptides to MHC-II and antigen presentation (Harding, 1991; Levine and Chain, 1991). As Δ*fbpA* phagosomes showed signs of enhanced maturation and activated receptor expression, experiments were performed to determine the efficacy of antigen presentation by Δ*fbpA* infected MΦs and DCs. We previously showed that MΦs infected with Δ*fbpA* triggered IFN-γ response from unpurified T cells from Mtb sensitized mice (Copenhaver *et al.*, 2004). In this study, we compared Δ*fbpA* infected MΦs and DCs for their ability to prime using CD3-bead purified T cells. Δ*fbpA* infected MΦs and DCs induced a stronger IFN-γ response from Mtb sensitized T cells from mice (supplemental data). Figure 9 illustrates the levels of IFN-γ released by sensitized T cells over 72 h when primed from either MΦs (Fig. 9A) or DCs (Fig. 9B). The wild-type H37Rv induced a poor IFN-γ response over the 3 day incubation while BCG showed a reduced ability to induce IFN-γ compared with Δ*fbpA* infected APCs. Furthermore, IL-12p70 levels were significantly higher in Δ*fbpA* APC–T cell co-cultures than either BCG or H37Rv co-cultures (Fig. 9C and D). Increased levels of IL-12 found in latter cultures is consistent with our previous observation that Δ*fbpA* enhanced IL-12 and IFN-γ mRNA expression in

mouse lungs during acute infection (Copenhaver *et al.*, 2004). Together, these data suggest that Δ*fbpA* drives a stronger Th1 response in mice compared with BCG or H37Rv.

Discussion

Mtb is internalized by MΦs through various receptors that may influence the fate of organisms (Ernst, 1998; Blander and Medzhitov, 2004). We found earlier that Δ*fbpA* mutant and wild-type Mtb differed in growth within MΦs although both were phagocytosed by MΦs equally well (Copenhaver *et al.*, 2004). In this study, we examined the molecular basis for the attenuation of Δ*fbpA* mutant that lacks the antigen 85A-mycoloyl transferase. Δ*fbpA* had reduced levels of TDM that led to a decreased synthesis of SOCS-1 in MΦs. SOCS-1 has emerged as a major regulator of cytokine-mediated antibacterial activity, TLR mediated signalling via IFN-γ in MΦs and maturation of DCs (O'Keefe *et al.*, 2001; Imai *et al.*, 2003; Bartz *et al.*, 2006). Consistent with this observation, MΦs activated even *after* infection with mycobacteria were better able to kill Δ*fbpA* than either BCG or wild-type H37Rv. This suggesting that Δ*fbpA* mutant was less suppressive for MΦs through reduced induction of SOCS-1.

Additional studies focused on mechanisms through which MΦs were able to contain Δ*fbpA* in comparison with BCG and H37Rv. ROS and NO constitute the major anti-mycobacterial mechanisms of MΦs and the growth of Δ*fbpA* mutant was enhanced by the blockade of ROS and NO, respectively, by DPI and NMMA (Fig. 3C). Interestingly, blockade of ROS enhanced the growth of Δ*fbpA* but not that of BCG or H37Rv while all three strains were affected by the blockade of NO. An additional explanation for the enhanced susceptibility of Δ*fbpA* to ROS was suggested by the *in situ* localization studies of oxidant enzymes around phagosomes in MΦs. *Phox* assembles from several different components ($p47^{phox}$, $p67^{phox}$, $gp91^{phox}$ and others) during the invagination and formation of the phagosome in MΦs and neutrophils (Babior, 1999). Phagosomal membrane *phox* then secretes copious amounts of superoxide into the lumen of the phagosomes which spontaneously dismutates into hydrogen peroxide (H_2O_2) (Suh *et al.*, 2006). The latter can in turn yield more bactericidal species such as hydroxyl radical and hypochlorous acid depending upon the iron and chloride ions available within the phagosomes. Our studies showed that Δ*fbpA* colocalized more with *phox* enzyme and therefore, we suggest that Δ*fbpA* is more susceptible to ROS (Figs 3 and 4). In support of this, virulent H37Rv phagosomes were found to exclude *phox* in MΦs (Fig. 4) (Daniel *et al.*, 2006), and superoxide dismutase defective strains of H37Rv were found more susceptible to oxidants (Edwards *et al.*, 2001). Similar considerations appear to apply to the increased tendency of Δ*fbpA* phagosomes to colocalize with iNOS as NO is a more powerful antimyco-bacterial agent (Fig. 4). In summary, Δ*fbpA* appears more susceptible to intracellular oxidants.

Recent studies show that cell wall lipids make a difference in the ability of mycobacteria to traffic within MΦs (Chua and Deretic, 2004; Chua *et al.*, 2004). Lipoarabiomannan has been found to interfere with phagosome maturation while TDM coated liposomes were reported to repulse each other *in vitro* alluding that it may affect endosome fusion within MΦs (Spargo *et al.*, 1991). Interestingly, a cord forming trahalose lipid defective mutant of *M. marium* was also reported to be defective in phago-some maturation (Robinson *et al.*, 2007). As Δ*fbpA* was TDM deficient, these considerations prompted us to examine its intracellular trafficking pattern. Traditionally, phagocytosed bacteria in MΦs are internalized into phagosomes that fuse with various types of early and late endosomes that deliver various cellular cargo and ultimately the phagosome fuses with lysosomes where bacterial degradation takes place owing to proteases and lipases (Gabay *et al.*, 1986) (Levine and Chain, 1991). Armstrong and Hart made the historical observation of that wild-type Mtb avoids destruction by avoiding P-L fusion that has been confirmed by others using wild-type

H37Rv as well as BCG (Armstrong and Hart, 1971; McDonough *et al.*, 1993; Clemens and Horwitz, 1995; Russell, 1995; Deretic and Fratti, 1999; Pieters, 2001; Kusner, 2005). However, Mtb and BCG phagosomes retain the selective ability to fuse with early endosomes acquiring molecules such as transferrin, transferrin receptor, organelles as well as MHC-II molecules (Clemens and Horwitz, 1996; Sturgill-Koszycki *et al.*, 1996; Russell, 2003). In addition, they acquire glycosphingolipids from MΦ plasma membrane through recycling endosomes. Finally, proteolytic enzymes such as Cathepsin-D (Cat-D) are delivered to their phagosomes although, owing to the exclusion of vacuolar protonATPase (vATPase) by Mtb, BCG and *M. avium* phagosomes, Cat-D remains inactive (Ullrich *et al.*, 1999).

These observations indicate that Mtb and BCG phagosomes fuse selectively with early endosomes to derive nutrients and organelles for growth but do not fuse with lysosomes to evade killing through degradation. Thus the 'maturation arrest' of Mtb and BCG facilitates their survival within MΦs. Using fluorescent endocytic tracers (LTR, TRR and MBR) we initially found that Δ*fbpA* phagosomes fused with early endosomes acquiring transferrin. However, unlike H37Rv or BCG, their phagosomes also showed an enhanced capacity to fuse with late endosomes containing either LTR or MBR probes. This suggested that the mutant was more fusion competent. We next investigated the molecular basis for enhanced endosomal fusion of Δ*fbpA* phagosomes and characterized whether P-L fusion occurred as a consequence.

Studies show that several *rab* GTPases regulate endosomal trafficking and early endosomes carry the *rab5* GTPase, recycling endosomes label for *rab11* while, lysosomes label for *rab7* and CD63. A number of downstream effector proteins such as early embryonic antigen 1 (EEA1), a protein that binds *rab5* and triggers the recruitment of phosphatidyl inositol-3 kinase (PI-3K), and Hepatocyte growth factor-regulated tyrosine kinase substrate (Hrs) are also involved in endosome fusion. Interestingly, Mtb and BCG phagosomes acquire *rab5*, an early endosomal docking protein while excluding *rab7,* a marker of lysosomes (Deretic *et al.*, 1997; Via *et al.*, 1997). More recent studies show that *rab5* to *rab7* conversion is defective on Mtb and BCG phagosomes preventing lysosomal fusion (Rink *et al.*, 2005). The defect in maturation also extends to the exclusion of downstream docking and sorting proteins. Thus, EEA1 is absent and levels of phosphatidyl inositol phosphate are reduced on Mtb phagosomes, and Hrs is defectively recruited by mycobacteria. In contrast, these markers are recruited actively and are abundant on inert latex bead phagosomes (Vergne *et al.*, 2004b; Vieira *et al.*, 2004; Deretic *et al.*, 2007).

The differential presence of *rab* and other docking proteins on early and recycling endososomes and lysosomes prompted us to analyse Δ*fbpA,* H37Rv and BCG phagosomes in MΦs. Δ*fbpA* phagosomes acquired *rab5A, rab5B* as well as *rab11* that appeared to explain their enhanced ability to fuse with 'early' and 'recycling' endosomes respectively (Vieira *et al.*, 2002). They also acquired the protein tyrosine kinase (Hck) a marker of late endosomes that seems to explain their ability to fuse with late endosomes (Astarie-Dequeker *et al.*, 2002). Paradoxically, Δ*fbpA* phagosomes consistently excluded *rab7* and CD63 markers of lysosomes. Thus, Δ*fbpA* phagosomes differed from H37Rv and BCG in being able to fuse with early, recycling as well as late endosomes but resembled them by avoiding lysosomal fusion. Together, these studies show that Δ*fbpA* phagosomes are more fusion competent than either BCG or H37Rv, have more maturation markers and are more susceptible to intracellular oxidants, attributing them a unique phenotype.

As Δ*fbpA* mutant was effective as a candidate vaccine, we investigated whether these features translated into an increased efficiency of antigen presentation (Copenhaver *et al.*, 2004). Antigen presentation consists of an intracellular component where bacteria are

degraded by proteases such as cathepsins in an acidic environment and the membrane expression of the MHC-II bound peptides in conjunction with costimulatory and adhesion molecules (Levine and Chain, 1991). The MHC-II forms an immunological synapse along with CD80, CD86 and CD40 to optimally present peptides to T cells (Harding, 1991; Levine and Chain, 1991). Δ*fbpA* enhanced the expression of MHC-II and costimulatory molecules on both MΦs and DCs. As SOCS-1 has been found to downregulate the MHC-II expression of MΦs, we suggest that the ability of Δ*fbpA* to enhance MHC-II expression is related to its reduced induction of SOCS-1 (Fig. 2). Finally, Δ*fbpA* infected MΦs and DCs were more efficient to induce a stronger recall IFN-γ response in the immune T cells of mice. We suggest that this was due to an increased expression of MHC-II as well as costimulatory molecules such as CD40 and CD86.

The unique behaviour of Δ*fbpA* in MΦs raised interesting questions on the essentiality and function of the genes encoding Ag85A, Ag85B and Ag85C. Following our initial report that *fbpA* disruption resulted in an attenuated phenotype, others showed that disruption of the gene encoding Ag85C (*fbpC*) also resulted in changes in cell wall permeability and fatty acid composition (Puech *et al.*, 2002). Subsequently, Ronning *et al.* (2004) reported that despite similarity in function, the amino acid residues near the substrate binding sites of Ag85 complex are different suggesting that all three were required for the optimal synthesis of TDM. We suggest that the deletion of *fbpA* led to a deficiency in TDM levels perhaps because its function could not be complemented by either *fbpB or fbpC* and this, in turn, led to its attenuation. That Δ*fbpA* is more essential for the survival of Mtb is also supported by the observation that antisense oligonucleotides against the *fbpA* mRNA inhibited Mtb growth in broth to a greater extent than oligonucleotides against mRNA from *fbpB or fbpC* (Harth *et al.*, 2002). Together, these studies indicate that *fbpA* is more essential for the virulence of Mtb despite being an important antigen inducing T cell responses (Ramachandra *et al.*, 2001). Furthermore, it is important to note that the *fbpB*-encoded Ag85B is a more significant immunodominant antigen of Mtb (Launois *et al.*, 1994). Initially identified to contain the immunodominant Th1 epitope ‘peptide 25’, Ag85B is an integral component of multiple successful DNA vaccines including those under clinical trials (Skeiky and Sadoff, 2006). Thus, we suggest that deletion of *fbpA* appears to have led not only to attenuation but also enhanced immunogenicity because of an altered intracellular behaviour in APCs and intact Ag85B. In conclusion, our studies suggest that the mechanisms through which a vaccine is processed in APCs may ultimately determine their efficacy and candidate antituberculosis vaccines perhaps need to be optimized for efficient processing by APCs.

Experimental procedures

Bacteria

The wild-type *M. tuberculosis* H37Rv and *Mycobacterium bovis* BCG (#35734) were from ATCC repository (MD, USA). The Δ*fbpA* and the reconstituted Δ*fbpA* mutant were prepared as described before (Armitige *et al.*, 2000). The green fluorescent protein (*gfp*)-expressing strains of Δ*fbpA*, H37Rv and BCG were prepared as per previously described techniques (Dhandayuthapani *et al.*, 1995). They were grown once in bulk in 7H9 broth without additives (H37Rv and BCG), Middlebrook 7H9 broth with 25 μg ml^{-1} kanamycin (D*fbp*) and 7H9 broth with 25 μg ml^{-1} kanamycin and 50 μg ml^{-1} hygromycin (*gfp*Δ*fbp*). After 7–10 days, bacteria were harvested, washed, sonically dispersed and stored in aliquots at –70°C. Infections were performed with freshly re-grown, washed, log phase organisms (day 7–10) generated from these single use seed aliquots. For fluorescence microscopy, gently sonicated single cell suspensions were used at an multiplicity of infection (moi) of 1:1. It should be noted that phagocytosis of multiple bacteria into MΦs did not affect their colocalization pattern unless they were large clumps.

Radiolabelled acetate incorporation assay for determination of cell wall TDM

Metabolic radiolabelling of Mtb and mutants—Δ*fbpA* mutant, the reconstituted Δ*fbpA* mutant and H37Rv strains were grown with continuous shaking for 7 days at 37°C (to late log phase) in 7H9 broth (20 ml) supplemented withADC enrichment containing 0.2% glucose and 1% glycerol. An aliquot of 5 ml was removed, turbidity adjusted to McFarland #1 standard and 40 μCi of sodium ^{14}C-acetate (57 mCi mmol^{-1}) (Amersham Pharmacia) added to tubes which were incubated for 3, 6, 12 and 24 h. Plating of McFarland #1 adjusted culture showed that the start inoculum contained 1×10^8 cfu ml^{-1} for the wild-type, Δ*fbpA* and reconstituted Δ*fbpA*. After radiolabelling, the cultures were harvested by centrifugation (5000 r.p.m. for 10 min) and the bacterial pellets were washed in cold PBS (three washes by centrifugation) and ethanol.

Extraction and analysis of radiolabelled TDM—The bacterial pellets were then extracted four times with 1 ml portions of chloroform-methanol (CM) 2:1. After centrifugation, the upper liquid phases (containing cell wall-bound mycolic acids) were collected. Extracts of the upper phases were pooled and dried in glass vials. These ^{14}C-acetate incorporated glycolipids were dissolved in 200 μl of CM (2:1), radioactivity determined by scintillation counting, and analysed for presence of radiolabelled TDM by TLC, autoradiography and phosporimage analysis.

TLC of TDM bands—The TDM mixtures were separated by TLC on silica gel 60 plates in solvent C. For radiolabelled glycolipid samples, about 40 000 c.p.m. per lane were applied. TLC standards of TDM (20 μg, Sigma Chemical, MO) were cochromatographed with the radiolabelled glycolipid samples. After separation, the TLC plates were allowed to dry, exposed to a scanning Storm phosphorimager, and radioactivity quantified by the use of ImageQuant software. For autoradiography, the TLC plates were exposed to photographic films for 24–48 h.

MΦs and DCs

C57BL/6-derived MΦs were cultured in McCoy's medium with 10% FBS, penicillin and gentamicin (medium) supplemented with 10 ng ml^{-1} recombinant mouse GM-CSF (Cell Sciences). MΦs were rested in GM-CSF-free medium for 2 days and used for mycobacterial infections. C57BL/6 bone marrow-derived macrophage-like cell line BMA.A3 was kindly provided by Dr Kenneth L. Rock (University of Massachusetts Medical School). This cell line maintained in the same medium, has been well characterized to study phagocytosis and antigen presentation by MTB (Teitelbaum *et al.*, 1999). Primary and cell line MΦs were maintained as monolayers in 24-well plates for growth curve determinations or oxidant assays, eight-well slide chambers for fluorescence microscopy or in 75 ml flasks for preparation of phagosomes during phagosome maturation studies. DCs were cultured from mouse bone marrow cells grown in GM-CSF and IL-4 containing medium for 7 days and CD11c+ cells purified using anti-CD11c-coated magnetic beads (Miltenyi, USA) as described by the manufacturer. The cells were more than 97% pure and contained a mix of CD8α+ and CD8α– DCs as described (Moulton *et al.*, 2007).

SOCS-1 signalling in MΦs after infection

MΦs were infected with mycobacteria at an moi of 1:1 and washed after 1 and 4 h. Lysates were estimated for protein content, mixed with an antiprotease mix and equal volumes loaded per lane and analysed by Western blot against a SOCS-1-specific antibody (Santa Cruz Biotechnology, USA). Bands were visualized using chemiluminiscence. MΦs were also activated with TDM suspension in mineral oil suspension or vehicle alone to determine SOCS-1 induction. Blots were probed with an antibody to β-actin to ensure equal protein

load in lanes. MΦs were separately stained using acid fast stain to confirm that they contained approximately equal numbers of intracellular mycobacteria (not shown).

Growth curves for Mtb or BCG strains in MΦs

These were carried out as described before (Copenhaver *et al.*, 2004; Daniel *et al.*, 2006) using organisms to infect naïve MΦs or BMA.3 cells (both yield similar results, data not shown) in 24-well format at an moi 1:1 and plating cfu on days 0, 3 and 7 post infection. To study the effect of MΦ activation on growth curves, in addition to naïve MΦs, replicates of MΦ cultures were activated with 400 U ml^{-1} of IFN-γ for 24 h prior to infection and cfu counts. MΦs were fully viable (> 90%) until day 7 as tested by alamar blue conversion method (Benghuzzi, 1995). The blockade of ROS and NO was achieved by incubating infected MΦs with 10 μM DPI a non-scavenging NADPH oxidase inhibitor or 50 mM NMMA an inhibitor of NO synthesis, or their combination (Lee *et al.*, 2005; Wang *et al.*, 2006). These doses were based on initial dose–response titrations to determine inhibition of ROS and NO respectively.

Localization of phox proteins and iNOS on phagosomes within MΦs using immunofluorescence

MΦs were infected with live *gfp*Δ*fbpA, gfpH* 37Rv or *gfp*BCG using eight-well chambers and stained for colocalization with goat antibodies to mouse $p47^{phox}$ (Santa Cruz Biotechnology, CA) or a mouse monoclonal antibody to mouse iNOS (Sigma Chemical, MO) using the protocol described earlier (Daniel *et al.*, 2006). Cells were mounted in Elvanol mountant and examined using a Deltavision LSM to confirm colocalization patterns and analysis of the staining patterns of anti-$p47^{phox}$ or iNOS antibodies. A positive control of phorbol myristyl acetate activated uninfected MΦs and a negative control consisting of uninfected, untreated and rested MΦs were stained with anti-$p47^{phox}$ antibodies for each type of MΦ and time point analysed. In addition, antibody isotype controls were included using *gfp*MTB-infected MΦs stained with normal goat or mouse IgG followed by Texas redconjugated antispecies IgG. Unactivated or uninfected MΦs presented a uniformly low background staining with this procedure. *phox*-specific staining on phagosomes was evident as dense tubular or spherical staining, strongly colocalizing with phagosomes (Daniel *et al.*, 2006). INOS-specific staining with the mab was more granular and localized in cytoplasm or around phagosomes. Per cent colocalization of *gfp*-mycobacteria with either *phox* or iNOS was determined by counting at least 100 fields of a quadruplicate slide chamber per mouse bone marrow-derived preparation and averaging the numbers. All scoring was blinded. The standard deviations were calculated from three independent experiments using MΦs from three mice in each experiment and *P*-value determined for colocalization scores using the *t*-test. It should be noted that after gentle sonication we obtained mostly a single cell suspension. However, occasional clumps of bacteria in MΦs were unavoidable and we eliminated such clumps from being scored for colocalization purposes. Furthermore, MΦ monolayers were washed four times with media to ensure that extracellular bacteria were not a problem. In our hands, when moi was below 1:5 such bacteria were rare.

Fluorescent immunostains for early, recycling and late endosome-lysosome markers on phagosomes

The immunostaining of MΦs infected with *gfp*-mycobacteria was carried out similar to the procedure described for *phox* proteins. The antibodies used were *rab5A, rab5B, rab11, rab7*, CD63, Hck and PI-3 kinase (Santa Cruz Biotechnology, CA). LAMP-1 (ID4B clone) was from the Developmental Hybrodoma Bank, IA).

Measurement of oxidant activity

Intracellular ROS using flow cytometry—BMA.A3 MΦs were infected with mycobacteria at an moi of 1:1 and washed after 4 h. The cells were suspended in 5 μM H_2DCFDA for 5 min, and analysed for intracellular fluorescence using a Cellquest software and BD-Facscan instrument. The non-fluorescent H_2DCFDA probe is cleaved within living cells by esterases and the resultant DCF is oxidized to DCFH by ROS produced within MΦs yielding a green fluorescent compound, which in turn, is trapped within cells by hydrophobic binding to cytoplasmic proteins. Histograms were analysed for MFIs in three independent experiments and *P*-value calculated using Student's *t*-test.

Quantitation of ROS using fluorometry—Superoxide generated by *phox* dismutates to yield H_2O_2 which can oxidize H_2DCFDA to a fluorescent product which can then be measured by fluorometry (Daniel *et al.*, 2006). BMA.A3 cells in 24 wells (10^6 cells per well; three wells were used for each strain) were infected with myco-bacteria as above for 4 h and washed. They were added with 100 μM H_2DCFDA and fluorescence in average fluorescence units (AFUs) quantified using an Ascent fluoroscan. AFUs from infected as well as control MΦs in three independent experiments were plotted against time.

Quantitation of NO using colorimetry—Nitrite derived from NO in medium of BMA.A3 MΦs infected as per ROS detection was quantified using Griess reagent and spectrophotometry as described before (Jagannath *et al.*, 1998).

Phagosomal acquisition of late endosomal markers

LTR labelling of late endosomes—LTR (DND99; Molecular probes Inc, Eugene OR) localizes in LAMP-1 positive late endosomes which do not fuse with live MTB containing phagosomes (Via *et al.*, 1998). Colocalization of green Mtb with red coloured LTR thus suggests phagosome-late endosome fusion. MΦs or BMA.A3 MΦs (both gave similar results) were preloaded with 1/1000 dilution of LTR for 4 h, washed and infected with *gfp*-mycobacterial strains for another 4 h. After another step of washing cells were incubated for and fixed cells were then examined at 24 h for phagosomal labelling of LTR using LSM.

MBR labelling of late endosomes—The late endosomes were created by endocytosing mannosylated BSA labelled with rhodamine (MBR; Sigma Chemical, MO). MBR enters through the MΦ mannose or lectin type receptors and matures from early to late endosomes in about 2 h (Astarie-Dequeker *et al.*, 1999). The latter have been reported to fuse with MTB phagosomes after activation with IFN-γ although live virulent Mtb has been reported to exclude this marker in unactivated MΦs (Kang *et al.*, 2005). MΦs were labelled with MBR for 2 h, washed twice with warm medium and infected with *gfp*-mycobacterial strains for 4 h before being washed again three times and re-incubated for another 24 h. Colocalization with MBR was also determined using LSM.

Labelling of MΦs with TRR—BMA.A3 MΦs were washed with serum-free McCoy medium and incubated with TRR at 5 μg ml^{-1} for 90 min. Cells were then washed and chased with complete medium three times for 120 min. MΦs were then infected with *gfp*-mycobacteria for 4 h, washed and incubated for another 24 h. MΦs were examined as above for colocalization. Per cent colocalization of LTR, MBR and TRR against *gfp*-mycobacteria was determined as described for *phox* and iNOS using similar numbers of mice.

Detection of phagosomal membrane proteins by immunoblot analysis

BMA.A3 MΦs were grown as monolayers in 75 ml flasks and infected at moi of 1:1–1:5 with mycobacteria for 4 h, washed and incubated for another 24 h. Mycobacterial

phagosomes were fractionated as per the procedures described by Ullrich *et al.* at the end of these time points (Ullrich *et al.*, 1999; Ullrich *et al.*, 2000). Briefly, 2 h before fractionation, MΦ monolayers were washed once with warm serum-free medium, gently scraped, washed three times in a fractionation buffer (PFB) with 10 mM Hepes, 5 mM EDTA, 5 mM EGTA, pH 7.0 and suspended in PFB with an antiprotease mix consisting of 1 μg ml^{-1} leupeptin, 1 μg ml^{-1} pepstatin and 1 mM phenylmethyl sulfonylfluoride. Pellets were then homogenized in a glass tissue homogenizer 10 times and passed 10 times through a 28-gauge needle. Lysates were centrifuged at 500 *g* for 5 min to sediment nuclei and the post nuclear supernatant was layered on a step gradient of 50% and 12% sucrose in PFB. After centrifugation at 1000 *g* for 60 min, the interphase of phagosome fraction was collected and further purified by passing through two successive cushions of 70 and 400 kDa ficoll in PFB as described before. The final purified phagosomal pellet was collected by centrifugation at 10 000 *g* for 15 min and suspended in SDS sample buffer and subjected to ultrasonic disruption for 5 min. Latex beads (IgG coated, 2 μM diameter, Sigma chemical, MO) were added into MΦs for 60 min, washed and phagosomes fractionated 4 h after phagocytosis as they mature earlier. Phago-some pellets were heated at 98°C for 5 min were then electro-phoresed using a 4–20% gradient SDS gel, electroblotted and membranes were probed with antibodies as used above for immunostains. Bands were visualized using a chemiluminiscence kit from Amersham. The post-nuclear supernatants obtained from MΦ lysates served as control cytosol preparations and were used to determine the basal level of endosome markers after estimation of protein (Ullrich *et al.*, 1999; Ullrich *et al.*, 2000). All the markers tested for phagosome analysis were found in cytosol of all MΦs infected with mycobacteria, but were present differentially on purified phagosome pellets, suggesting that phagosomal translocation was dependent on the phagocytosed material.

Antigen presentation assay

The methods have been previously described (Copenhaver *et al.*, 2004; Connelly *et al.*, 2007; Moulton *et al.*, 2007). Sensitized and naïve T cells were derived from C57BL/6 mice. One group of mice was left un-immunized (naïve) and another group was immunized via subcutaneous route with one dose of H37Rv given at the base of tail 2 weeks apart. Mice were then treated with an oral dose of INH (25 mg kg^{-1}) for 10 days and mice were sacrificed 3 days after the last drug dose. Spleen cells were gently teased apart, suspended in ACK buffer to lyse red cells, washed and incubated in RPMI-1640 medium with 10% FBS (medium) for 24 h for monocytes to adhere. CD3+ bead purified T cells were fractionated using magnetic columns (Miltenyi, USA) and layered on APCs. APCs infected with Δ*fbpA*, H37Rv or BCG were separately overlaid with H37Rv sensitized T cells and the supernatants collected to determine the cytokine levels. To generate APCs, bone marrow-derived adherent MΦs cultured in GM-CSF containing medium for 7 days were infected with H37Rv bacteria or left uninfected as monolayers in 24-well plates. The DCs were obtained by culturing bone marrow cells for 7 days in medium with GM-CSF and IL-4 (10 ng ml^{-1} each) and purifying CD11c+ cells through a magnetic column. The cells were routinely 98% pure and were used as such as immature DCs without additional activation (Moulton *et al.*, 2007). The DCs were also infected with mycobacteria at an moi of 1:1. After a 4 h infection, monolayers of MΦs or DCs were washed extensively to remove non-phagocytosed bacteria and overlaid with T cells. For both MΦ and DC co-cultures, T cells were overlaid at a ratio of 1:20. For each type of APCs on the monolayer, triplicate wells were overlaid with T cells from three H37Rv immunized mice and naive splenocytes from three unimmunized mice. Twenty-four, 48 and 72 h after the addition of T cells, 200 μl aliquots of supernatants were collected from each well of the APCs along with control wells leaving behind 400 μl at the end of 72 h when supernatant collections were terminated. Medium was not replenished as no loss of viability was detected among T cells in pilot experiments and viability was

measured of the APC/T-cell overlay using Alamar blue viability indicator. IFN-γ or IL-12p70 in the medium was determined using sandwich ELISA kits from R&D (USA).

Acknowledgments

The authors wish to thank the NIH for supporting these studies through the NIAID AI49534 grant. We are grateful for the kind gift of BMA.A3 cell line by Dr Kenneth L. Rock, University of Massachusetts, USA. Dr Katti was supported by a fellowship from the Department of Biotechnology, Ministry of Health, Government of India.

References

Armitige LY, Jagannath C, Wanger AR, Norris SJ. Disruption of the genes encoding antigen 85A and antigen 85B of *Mycobacterium tuberculosis* H37Rv: effect on growth in culture and in macrophages. Infect Immun. 2000; 68:767–778. [PubMed: 10639445]

Armstrong JA, Hart PD. Response of cultured macrophages to *Mycobacterium tuberculosis*, with observations on fusion of lysosomes with phagosomes. J Exp Med. 1971; 134:713–740. [PubMed: 15776571]

Astarie-Dequeker C, N'Diaye EN, Le Cabec V, Rittig MG, Prandi J, Maridonneau-Parini I. The mannose receptor mediates uptake of pathogenic and nonpathogenic mycobacteria and bypasses bactericidal responses in human macrophages. Infect Immun. 1999; 67:469–477. [PubMed: 9916047]

Astarie-Dequeker C, Carreno S, Cougoule C, Maridonneau-Parini I. The protein tyrosine kinase Hck is located on lysosomal vesicles that are physically and functionally distinct from CD63-positive lysosomes in human macrophages. J Cell Sci. 2002; 115:81–89. [PubMed: 11801726]

Babior BM. NADPH oxidase: an update. Blood. 1999; 93:1464–1476. [PubMed: 10029572]

Banaiee N, Kincaid EZ, Buchwald U, Jacobs WR Jr, Ernst JD. Potent inhibition of macrophage responses to IFN-gamma by live virulent *Mycobacterium tuberculosis* is independent of mature mycobacterial lipo-proteins but dependent on TLR2. J Immunol. 2006; 176:3019–3027. [PubMed: 16493060]

Bartz H, Avalos NM, Baetz A, Heeg K, Dalpke AH. Involvement of suppressors of cytokine signaling in toll-like receptor-mediated block of dendritic cell differentiation. Blood. 2006; 108:4102–4108. [PubMed: 16896155]

Belisle JT, Vissa VD, Sievert T, Takayama K, Brennan PJ, Besra GS. Role of the major antigen of *Mycobacterium tuberculosis* in cell wall biogenesis. Science. 1997; 276:1420–1422. [PubMed: 9162010]

Benghuzzi HA. The role of various biomedical polymers concentration on the adhesion rate and viability of monocyte and monocyte derived macrophages. Biomed Sci Instrum. 1995; 31:121–126. [PubMed: 7654948]

Blander JM, Medzhitov R. Regulation of phagosome maturation by signals from toll-like receptors. Science. 2004; 304:1014–1018. [PubMed: 15143282]

Brewer TF, Colditz GA. Relationship between bacille Calmette-Guerin (BCG) strains and the efficacy of BCG vaccine in the prevention of tuberculosis. Clin Infect Dis. 1995; 20:126–135. [PubMed: 7727638]

Chua J, Deretic V. *Mycobacterium tuberculosis* reprograms waves of phosphatidylinositol 3-phosphate on phagosomal organelles. J Biol Chem. 2004; 279:36982–36992. [PubMed: 15210698]

Chua J, Vergne I, Master S, Deretic V. A tale of two lipids: *Mycobacterium tuberculosis* phagosome maturation arrest. Curr Opin Microbiol. 2004; 7:71–77. [PubMed: 15036144]

Clemens DL. Characterization of the *Mycobacterium tuberculosis* phagosome. Trends Microbiol. 1996; 4:113–118. [PubMed: 8868090]

Clemens DL, Horwitz MA. Characterization of the *Mycobacterium tuberculosis* phagosome and evidence that phagosomal maturation is inhibited. J Exp Med. 1995; 181:257–270. [PubMed: 7807006]

Clemens DL, Horwitz MA. The *Mycobacterium tuberculosis* phagosome interacts with early endosomes and is accessible to exogenously administered transferrin. J Exp Med. 1996; 184:1349–1355. [PubMed: 8879207]

Connelly MA, Moulton RA, Smith AK, Lindsey DR, Sinha M, Wetsel RA, Jagannath C. Mycobacteria-primed macrophages and dendritic cells induce an up-regulation of complement C5a anaphylatoxin receptor (CD88) in CD3+ murine T cells. J Leukoc Biol. 2007; 81:212–220. [PubMed: 16997854]

Copenhaver RH, Sepulveda E, Armitige LY, Actor JK, Wanger A, Norris SJ, et al. A mutant of *Mycobacterium tuberculosis* H37Rv that lacks expression of antigen 85A is attenuated in mice but retains vaccinogenic potential. Infect Immun. 2004; 72:7084–7095. [PubMed: 15557632]

Daniel DS, Dai G, Singh CR, Lindsey DR, Smith AK, Dhandayuthapani S, et al. The reduced bactericidal function of complement C5-deficient murine macrophages is associated with defects in the synthesis and delivery of reactive oxygen radicals to mycobacterial phagosomes. J Immunol. 2006; 177:4688–4698. [PubMed: 16982908]

Deretic V, Fratti RA. *Mycobacterium tuberculosis* phagosome. Mol Microbiol. 1999; 31:1603–1609. [PubMed: 10209735]

Deretic V, Via LE, Fratti RA, Deretic D. Mycobacterial phagosome maturation, rab proteins, and intracellular trafficking. Electrophoresis. 1997; 18:2542–2547. [PubMed: 9527483]

Deretic V, Vergne I, Chua J, Master S, Singh SB, Fazio JA, Kyei G. Endosomal membrane traffic: convergence point targeted by *Mycobacterium tuberculosis* and HIV. Cell Microbiol. 2004; 6:999–1009. [PubMed: 15469429]

Deretic V, Singh S, Master S, Kyei G, Davis A, Naylor J, et al. Phosphoinositides in phagolysosome and autophagosome biogenesis. Biochem Soc Symp. 2007; 74:141–148. [PubMed: 17233587]

Dhandayuthapani S, Via LE, Thomas CA, Horowitz PM, Deretic D, Deretic V. Green fluorescent protein as a marker for gene expression and cell biology of mycobacterial interactions with macrophages. Mol Microbiol. 1995; 17:901–912. [PubMed: 8596439]

Donald PR, Maher D, Qazi S. A research agenda to promote the management of childhood tuberculosis within national tuberculosis programmes. Int J Tuberc Lung Dis. 2007; 11:370–380. [PubMed: 17394681]

Edwards KM, Cynamon MH, Voladri RK, Hager CC, DeStefano MS, Tham KT, et al. Iron-cofactored superoxide dismutase inhibits host responses to *Mycobacterium tuberculosis*. Am J Respir Crit Care Med. 2001; 164:2213–2219. [PubMed: 11751190]

Ernst JD. Macrophage receptors for *Mycobacterium tuberculosis*. Infect Immun. 1998; 66:1277–1281. [PubMed: 9529042]

Fine PE. The BCG story: lessons from the past and implications for the future. Rev Infect Dis. 1989; 11(Suppl. 2):S353–S359. [PubMed: 2652252]

Fine PE. BCG: the challenge continues. Scand J Infect Dis. 2001; 33:243–245. [PubMed: 11345212]

Fol M, Chauhan A, Nair NK, Maloney E, Moomey M, Jagannath C, et al. Modulation of *Mycobacterium tuberculosis* proliferation by MtrA, an essential two-component response regulator. Mol Microbiol. 2006; 60:643–657. [PubMed: 16629667]

Fratti RA, Vergne I, Chua J, Skidmore J, Deretic V. Regulators of membrane trafficking and *Mycobacterium tuberculosis* phagosome maturation block. Electrophoresis. 2000; 21:3378–3385. [PubMed: 11079558]

Fratti RA, Chua J, Deretic V. Induction of p38 mitogen-activated protein kinase reduces early endosome autoantigen 1 (EEA1) recruitment to phagosomal membranes. J Biol Chem. 2003; 278:46961–46967. [PubMed: 12963735]

Gabay JE, Horwitz MA, Cohn ZA. Phagosome-lysosome fusion. Biochem Soc Trans. 1986; 14:256–257. [PubMed: 3709950]

Gagliardi MC, Teloni R, Giannoni F, Pardini M, Sargentini V, Brunori L, et al. *Mycobacterium bovis* Bacillus Calmette-Guerin infects DC-SIGN-dendritic cell and causes the inhibition of IL-12 and the enhancement of IL-10 production. J Leukoc Biol. 2005; 78:106–113. [PubMed: 15845642]

Gercken J, Pryjma J, Ernst M, Flad HD. Defective antigen presentation by *Mycobacterium tuberculosis*-infected monocytes. Infect Immun. 1994; 62:3472–3478. [PubMed: 8039918]

Gioffre A, Infante E, Aguilar D, Santangelo MP, Klepp L, Amadio A, et al. Mutation in mce operons attenuates *Mycobacterium tuberculosis* virulence. Microbes Infect. 2005; 7:325–334. [PubMed: 15804490]

Harding CV. Pathways of antigen processing. Curr Opin Immunol. 1991; 3:3–9. [PubMed: 2054112]

Harries AD, Dye C. Tuberculosis. Ann Trop Med Parasitol. 2006; 100:415–431. [PubMed: 16899146]

Harth G, Horwitz MA, Tabatadze D, Zamecnik PC. Targeting the *Mycobacterium tuberculosis* 30/32-kDa mycolyl transferase complex as a therapeutic strategy against tuberculosis: proof of principle by using antisense technology. Proc Natl Acad Sci USA. 2002; 99:15614–15619. [PubMed: 12427974]

Imai K, Kurita-Ochiai T, Ochiai K. *Mycobacterium bovis* bacillus Calmette-Guerin infection promotes SOCS induction and inhibits IFN-gamma-stimulated JAK/STAT signaling in J774 macrophages. FEMS Immunol Med Microbiol. 2003; 39:173–180. [PubMed: 14625101]

Jagannath C, Actor JK, Hunter RL Jr. Induction of nitric oxide in human monocytes and monocyte cell lines by *Mycobacterium tuberculosis*. Nitric Oxide. 1998; 2:174–186. [PubMed: 9731635]

Kang PB, Azad AK, Torrelles JB, Kaufman TM, Beharka A, Tibesar E, et al. The human macrophage mannose receptor directs *Mycobacterium tuberculosis* lipoarabinomannan-mediated phagosome biogenesis. J Exp Med. 2005; 202:987–999. [PubMed: 16203868]

Kusner DJ. Mechanisms of mycobacterial persistence in tuberculosis. Clin Immunol. 2005; 114:239–247. [PubMed: 15721834]

Launois P, DeLeys R, Niang MN, Drowart A, Andrien M, Dierckx P, et al. T-cell-epitope mapping of the major secreted mycobacterial antigen Ag85A in tuberculosis and leprosy. Infect Immun. 1994; 62:3679–3687. [PubMed: 7520418]

Lee NK, Choi YG, Baik JY, Han SY, Jeong DW, Bae YS, et al. A crucial role for reactive oxygen species in RANKL-induced osteoclast differentiation. Blood. 2005; 106:852–859. [PubMed: 15817678]

Levine TP, Chain BM. The cell biology of antigen processing. Crit Rev Biochem Mol Biol. 1991; 26:439–473. [PubMed: 1722142]

Manca C, Tsenova L, Freeman S, Barczak AK, Tovey M, Murray PJ, et al. Hypervirulent *M. tuberculosis* W/Beijing strains upregulate type I IFNs and increase expression of negative regulators of the Jak-Stat pathway. J Interferon Cytokine Res. 2005; 25:694–701. [PubMed: 16318583]

McDonough KA, Kress Y, Bloom BR. Pathogenesis of tuberculosis: interaction of *Mycobacterium tuberculosis* with macrophages. Infect Immun. 1993; 61:2763–2773. [PubMed: 8514378]

McKinney JD, Honer zu Bentrup K, Munoz-Elias EJ, Miczak A, Chen B, Chan WT, et al. Persistence of *Mycobacterium tuberculosis* in macrophages and mice requires the glyoxylate shunt enzyme isocitrate lyase. Nature. 2000; 406:735–738. [PubMed: 10963599]

Miller BH, Fratti RA, Poschet JF, Timmins GS, Master SS, Burgos M, et al. Mycobacteria inhibit nitric oxide synthase recruitment to phagosomes during macrophage infection. Infect Immun. 2004; 72:2872–2878. [PubMed: 15102799]

Mommaas AM, Mulder AA, Out CJ, Girolomoni G, Koerten HK, Vermeer BJ, Koning F. Distribution of HLA class II molecules in epidermal Langerhans cells *in situ*. Eur J Immunol. 1995; 25:520–525. [PubMed: 7875214]

Moulton R, Connelly M, Smith K, Lindsey D, Haviland D, Wetsel R, et al. Complement C5a is an innate determinant of dendritic cell induced Th1 immunity to *Mycobacterium bovis* BCG infection in mice. J Leucocyte Biology. 2007; 82:956–967.

Nathan CF. Mechanisms of macrophage antimicrobial activity. Trans R Soc Trop Med Hyg. 1983; 77:620–630. [PubMed: 6362115]

Noss EH, Harding CV, Boom WH. *Mycobacterium tuberculosis* inhibits MHC class II antigen processing in murine bone marrow macrophages. Cell Immunol. 2000; 201:63–74. [PubMed: 10805975]

O'Keefe GM, Nguyen VT, Ping Tang LL, Benveniste EN. IFN-gamma regulation of class II transactivator promoter IV in macrophages and microglia: involvement of the suppressors of cytokine signaling-1 protein. J Immunol. 2001; 166:2260–2269. [PubMed: 11160280]

Pancholi P, Mirza A, Bhardwaj N, Steinman RM. Sequestration from immune CD4+ T cells of mycobacteria growing in human macrophages. Science. 1993; 260:984–986. [PubMed: 8098550]

Perskvist N, Long M, Stendahl O, Zheng L. *Mycobacterium tuberculosis* promotes apoptosis in human neutrophils by activating caspase-3 and altering expression of Bax/Bcl-xL via an oxygen-dependent pathway. J Immunol. 2002a; 168:6358–6365. [PubMed: 12055253]

Perskvist N, Roberg K, Kulyte A, Stendahl O. Rab5a GTPase regulates fusion between pathogen-containing phagosomes and cytoplasmic organelles in human neutrophils. J Cell Sci. 2002b; 115:1321–1330. [PubMed: 11884531]

Pieters J. Entry and survival of pathogenic mycobacteria in macrophages. Microbes Infect. 2001; 3:249–255. [PubMed: 11358719]

Puech V, Guilhot C, Perez E, Tropis M, Armitige LY, Gicquel B, Daffe M. Evidence for a partial redundancy of the fibronectin-binding proteins for the transfer of mycoloyl residues onto the cell wall arabinogalactan termini of *Mycobacterium tuberculosis*. Mol Micro-biol. 2002; 44:1109–1122.

Ramachandra L, Noss E, Boom WH, Harding CV. Processing of *Mycobacterium tuberculosis* antigen 85B involves intraphagosomal formation of peptide-major histocompatibility complex II complexes and is inhibited by live bacilli that decrease phagosome maturation. J Exp Med. 2001; 194:1421–1432. [PubMed: 11714749]

Rink J, Ghigo E, Kalaidzidis Y, Zerial M. Rab conversion as a mechanism of progression from early to late endosomes. Cell. 2005; 122:735–749. [PubMed: 16143105]

Robinson N, Wolke M, Ernestus K, Plum G. A mycobacterial gene involved in synthesis of an outer cell envelope lipid is a key factor in prevention of phagosome maturation. Infect Immun. 2007; 75:581–591. [PubMed: 17088345]

Ronning DR, Vissa V, Besra GS, Belisle JT, Sacchettini JC. *Mycobacterium tuberculosis* antigen 85A and 85C structures confirm binding orientation and conserved substrate specificity. J Biol Chem. 2004; 279:36771–36777. [PubMed: 15192106]

Russell DG. *Mycobacterium* and *Leishmania*: stowaways in the endosomal network. Trends Cell Biol. 1995; 5:125–128. [PubMed: 14732168]

Russell DG. What does ‘inhibition of phagosomelysosome fusion’ really mean? Trends Microbiol. 1998; 6:212–214. [PubMed: 9675795]

Russell DG. *Mycobacterium tuberculosis*: here today, and here tomorrow. Nat Rev Mol Cell Biol. 2001; 2:569–577. [PubMed: 11483990]

Russell DG. Phagosomes, fatty acids and tuberculosis. Nat Cell Biol. 2003; 5:776–778. [PubMed: 12951608]

Sambandamurthy VK, Wang X, Chen B, Russell RG, Derrick S, Collins FM, et al. A pantothenate auxotroph of *Mycobacterium tuberculosis* is highly attenuated and protects mice against tuberculosis. Nat Med. 2002; 8:1171–1174. [PubMed: 12219086]

Sambandamurthy VK, Derrick SC, Hsu T, Chen B, Larsen MH, Jalapathy KV, et al. *Mycobacterium tuberculosis* DeltaRD1 DeltapanCD: a safe and limited replicating mutant strain that protects immunocompetent and immunocompromised mice against experimental tuberculosis. Vaccine. 2006; 24:6309–6320. [PubMed: 16860907]

Scherer TA, Lauredo IT, Abraham WM. Scavenging of reactive oxygen species by a glycolipid fraction of *Mycobacterium avium* serovar 2. Free Radic Biol Med. 1997; 22:561–565. [PubMed: 8981049]

Singh CR, Moulton RA, Armitige LY, Bidani A, Snuggs M, Dhandayuthapani S, et al. Processing and presentation of a mycobacterial antigen 85B epitope by murine macrophages is dependent on the phagosomal acquisition of vacuolar proton ATPase and *in situ* activation of cathepsin D. J Immunol. 2006; 177:3250–3259. [PubMed: 16920965]

Skeiky YA, Sadoff JC. Advances in tuberculosis vaccine strategies. Nat Rev Microbiol. 2006; 4:469–476. [PubMed: 16710326]

Spargo BJ, Crowe LM, Ioneda T, Beaman BL, Crowe JH. Cord factor (alpha,alpha-trehalose 6,6′-dimycolate) inhibits fusion between phospholipid vesicles. Proc Natl Acad Sci USA. 1991; 88:737–740. [PubMed: 1992465]

Stewart GR, Wilkinson KA, Newton SM, Sullivan SM, Neyrolles O, Wain JR, et al. Effect of deletion or overexpression of the 19-kilodalton lipoprotein Rv3763 on the innate response to *Mycobacterium tuberculosis*. Infect Immun. 2005; 73:6831–6837. [PubMed: 16177361]

Sturgill-Koszycki S, Schaible UE, Russell DG. *Mycobacterium*-containing phagosomes are accessible to early endosomes and reflect a transitional state in normal phagosome biogenesis. EMBO J. 1996; 15:6960–6968. [PubMed: 9003772]

Suh CI, Stull ND, Li XJ, Tian W, Price MO, Grinstein S, et al. The phosphoinositide-binding protein p40phox activates the NADPH oxidase during FcgammaIIA receptor-induced phagocytosis. J Exp Med. 2006; 203:1915–1925. [PubMed: 16880255]

Teitelbaum R, Cammer M, Maitland ML, Freitag NE, Condeelis J, Bloom BR. Mycobacterial infection of macrophages results in membrane-permeable phagosomes. Proc Natl Acad Sci USA. 1999; 96:15190–15195. [PubMed: 10611360]

Ullrich HJ, Beatty WL, Russell DG. Direct delivery of procathepsin D to phagosomes: implications for phagosome biogenesis and parasitism by *Mycobacterium*. Eur J Cell Biol. 1999; 78:739–748. [PubMed: 10569246]

Ullrich HJ, Beatty WL, Russell DG. Interaction of *Mycobacterium avium*-containing phagosomes with the antigen presentation pathway. J Immunol. 2000; 165:6073–6080. [PubMed: 11086039]

Vazquez-Torres A, Fang FC. Salmonella evasion of the NADPH phagocyte oxidase. Microbes Infect. 2001; 3:1313–1320. [PubMed: 11755420]

Vergne I, Chua J, Singh SB, Deretic V. Cell biology of *Mycobacterium tuberculosis* phagosome. Annu Rev Cell Dev Biol. 2004a; 20:367–394. [PubMed: 15473845]

Vergne I, Fratti RA, Hill PJ, Chua J, Belisle J, Deretic V. *Mycobacterium tuberculosis* phagosome maturation arrest: mycobacterial phosphatidylinositol analog phosphatidylinositol mannoside stimulates early endosomal fusion. Mol Biol Cell. 2004b; 15:751–760. [PubMed: 14617817]

Via LE, Deretic D, Ulmer RJ, Hibler NS, Huber LA, Deretic V. Arrest of mycobacterial phagosome maturation is caused by a block in vesicle fusion between stages controlled by rab5 and rab7. J Biol Chem. 1997; 272:13326–13331. [PubMed: 9148954]

Via LE, Fratti RA, McFalone M, Pagan-Ramos E, Deretic D, Deretic V. Effects of cytokines on mycobacterial phagosome maturation. J Cell Sci. 1998; 111(Pt 7):897–905. [PubMed: 9490634]

Vieira OV, Botelho RJ, Grinstein S. Phagosome maturation: aging gracefully. Biochem J. 2002; 366:689–704. [PubMed: 12061891]

Vieira OV, Harrison RE, Scott CC, Stenmark H, Alexander D, Liu J, et al. Acquisition of Hrs, an essential component of phagosomal maturation, is impaired by mycobacteria. Mol Cell Biol. 2004; 24:4593–4604. [PubMed: 15121875]

Wang Y, Zeigler MM, Lam GK, Hunter MG, Eubank TD, Khramtsov VV, et al. The Role of the NADPH oxidase complex, p38 MAPK and Akt in regulating human monocyte/macrophage survival. Am J Respir Cell Mol Biol. 2006; 36:68–77. [PubMed: 16931806]

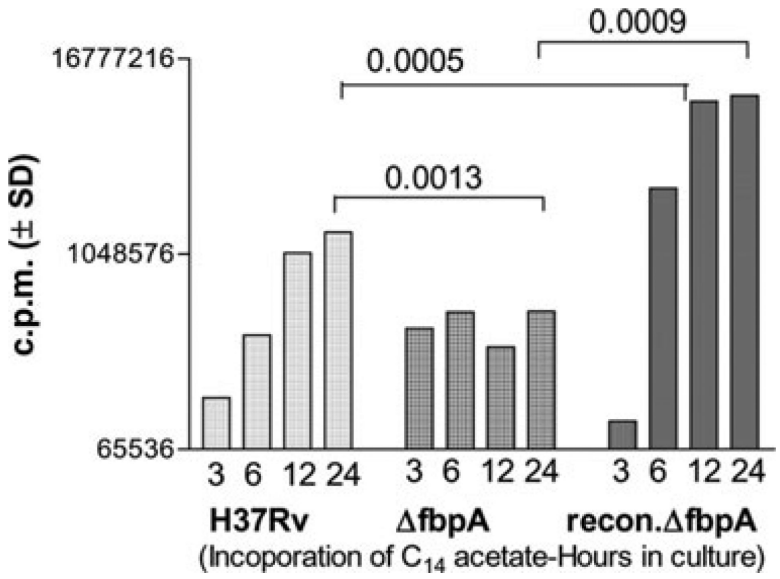

Fig. 1.

Disruption of *fbpA* gene leads to reduced cell wall lipids in Δ*fbpA* mutant compared with wild-type *Mycobacterium tuberculosis* (Mtb, H37Rv) and reconstituted Δ*fbpA*. Bacteria were grown in the presence of ^{14}C-acetate in 7H9 broth and at hourly intervals thin layer chromatographic analysis of cell wall extracts was performed followed by radiography. The bars represent c.p.m. ± SD (not apparent) of two similar experiments. Wild-type H37Rv incorporates more label than Δ*fbpA* mutant and the reconstitution of the gene restores the incorporation of radiolabel into the mutant (*P*-values shown for strains compared; Student's *t*-test).

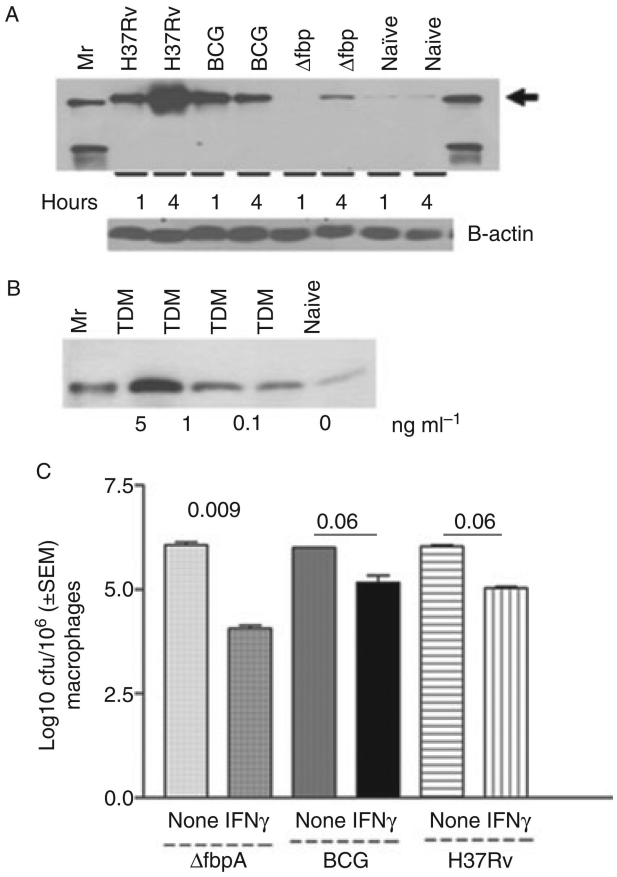

Fig. 2.

Δ*fbpA* affects signal transduction in MΦs through the delayed induction of suppressor of cytokine signalling 1 (SOCS-1).

A. ΔfbpA induces less strong SOCS-1 response. C57BL/6 mouse bone marrow-derived macrophages (MΦs) were infected with mycobacteria at an moi of 1:1 and incubated for 1 and 4 h. MΦ lysates were analysed using 7–12% SDS gels and electroblotted membranes were probed with an antibody to SOCS-1, followed by HRP-conjugate. Bands were detected using ECL. H37Rv and BCG induce copious expression of SOCS-1 in MΦs 1 and 4 h after infection. Δ*fbpA* does not induce SOCS-1 at 1 h but relatively lower levels of SOCS-1 are apparent at 4 h post infection (Mr, molecular weight marker). Lanes were loaded with equal amounts of protein as indicated by β-actin control.

B. Purified trehalose 6,6, dimycolate (TDM) induces SOCS-1. Varying amounts of TDM suspension in mineral oil were added to MΦs and lysates examined at 1 h after treatment for SOCS-1 as above. Naïve MΦs were treated with mineral oil control.

C. ΔfbpA is more susceptible to IFN-γ. MΦs were infected with mycobacteria (moi 1:1), washed to remove extracellular bacteria and 4 h later incubated with 400 U ml^{-1} of IFN-γ. 48 h later, the MΦs were lysed and plated for colony-forming unit (cfu) counts on 7H11 agar. Data summarizing three separate experiments show that IFN-γ is more effective in reducing the cfu of Δ*fbpA* when compared with its effects on MΦs infected with either BCG or H37Rv (*P*-values shown for groups compared; Student's *t*-test).

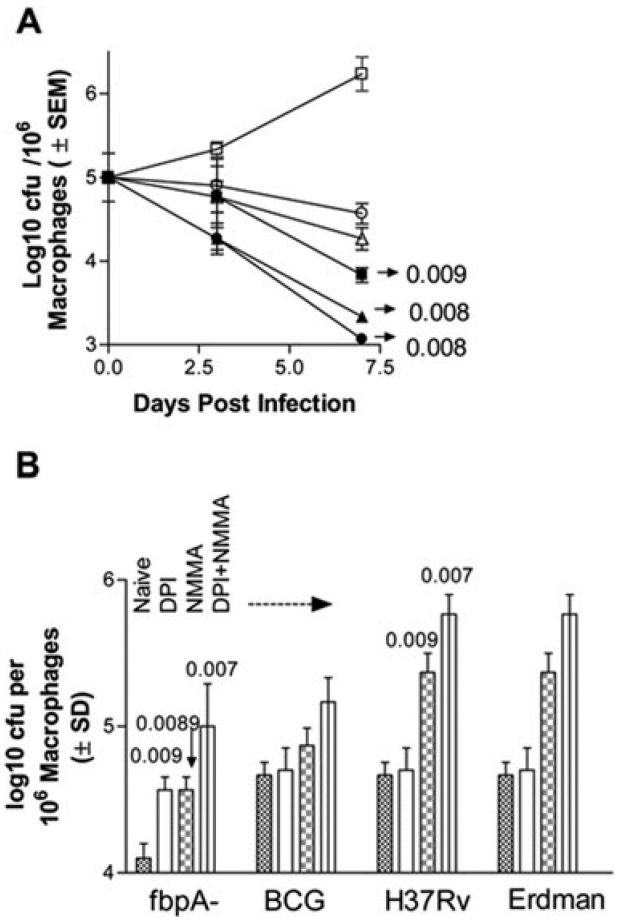

Fig. 3.

Growth and susceptibility of Δ*fbpA* mutant, H37Rv and BCG vaccine to intracellular oxidants.

A. Untreated (open symbols) or IFN-γ activated MΦs (closed symbols; 400 U ml^{-1} for 24 h) were infected with the three strains of mycobacteria and incubated. On days shown, triplicate wells of MΦs per strain were lysed and plated for cfu on 7H11 agar in three separate experiments. Δ*fbpA* (Δ) and BCG (○) are unable to grow while the wild-type H37Rv (□) shows an increase in cfu counts over 7 days. IFN-γ activation of MΦs decreases the cfu of all three strains by more than 1.5 $\log_{10}$ (*P*-values for growth in naïve MΦs versus IFN-γ activated MΦs; Student's *t*-test).

B. MΦs were infected as above and cfu determined on day 3 (see *Results*) in the presence or absence of an inhibitor of reactive oxygen species (ROS; diphenylene iodonium, DPI) or nitric oxide (NO) synthesis (NG-monomethyl-l-arginine, NMMA) or their combination. DPI and NMMA enhance the growth of Δ*fbpA*. DPI is ineffective against H37Rv while NMMA is effective. BCG shows a modest increase in growth with a combination of DPI and NMMA (*P*-values are shown above the bars versus growth of mycobacteria in naïve MΦs; Student's *t*-test). MΦs infected with Erdman strain show a growth profile similar to H37Rv and was included as another positive control.

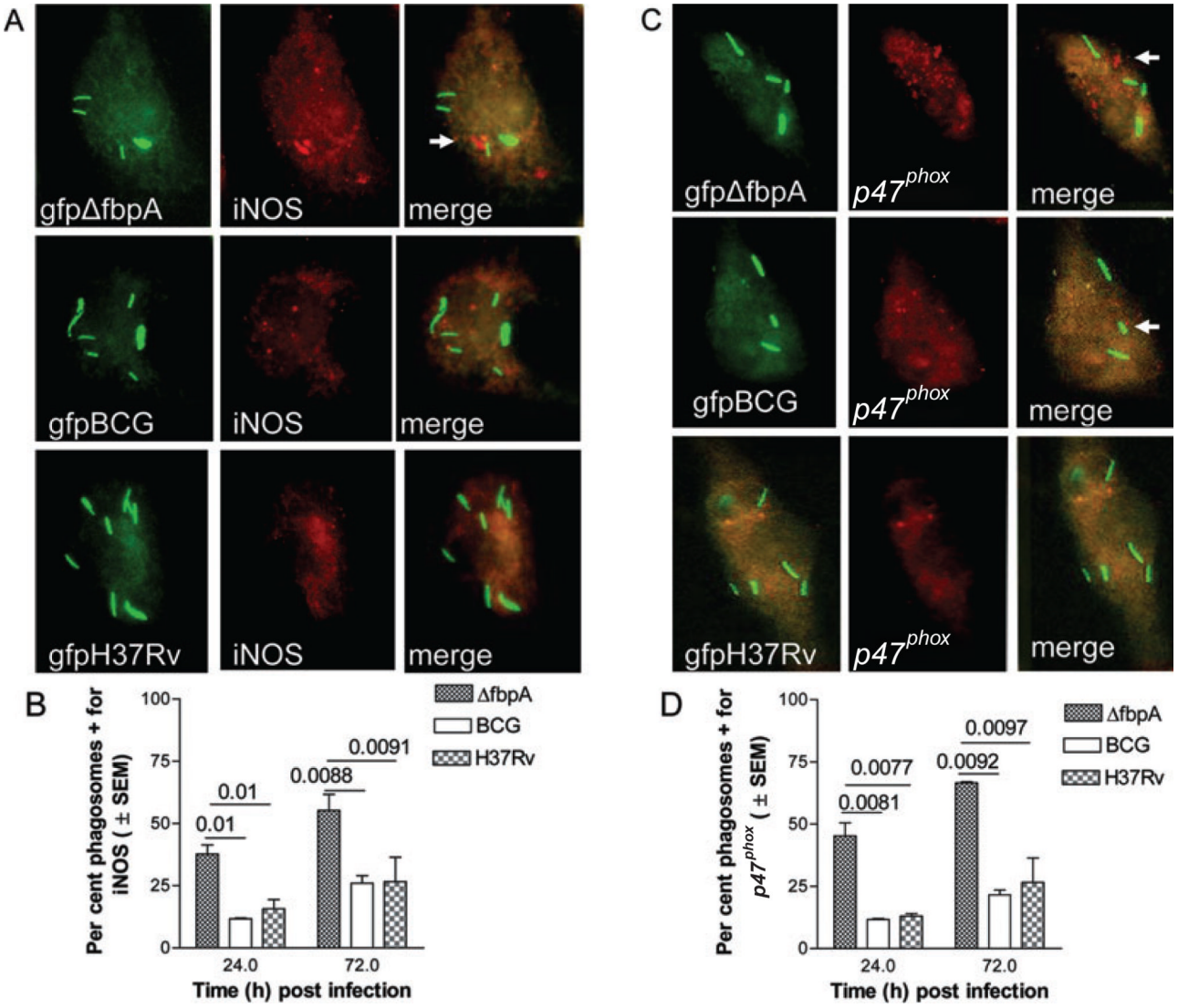

Fig. 4.

Phagosomes of Δ*fbpA* more frequently acquire inducible nitric oxide synthase (iNOS) and *p47*^{phox} component of phagocyte oxidase in MΦs. MΦs were infected with green fluorescent protein (*gfp*) expressing mycobacterial strains (*gfp*D*fbpA, gfp*BCG and *gfpH* 37Rv) for 4 h, washed and incubated for 24 or 72 h. MΦs were then fixed, permeabilized and stained with a mouse monoclonal antibody to iNOS or goat anti-*p47*^{phox} followed by anti-Ig-Texas red conjugates. MΦs were examined for colocalization using a Deltavision laser scanning microscope (LSM). Arrows illustrate colocalization in A and C.

A. LSM profiles illustrate that *gfp*Δ*fbpA* phagosomes acquire iNOS while *gfpH* 37Rv and *gfp*BCG acquire less.

B. Per cent phagosomes positive for iNOS colocalization was tabulated from three experiments and *P*-values are shown for the difference between *gfp*D*fbpA, gfp*DBCG and *gfpH 37Rv* phagosomes (Student's *t*-test). At least 200 microscopic fields were scored blind per mouse MΦ preparation. Colocalizing bacteria were averaged from three independent experiments each with MΦs from three mice; each microscopic field contained about five MΦs, each of which contained about five bacilli.

C. *gfp*Δ*fbpA* phagosomes acquire more *p47*^{phox} than either *gfpH* 37Rv or *gfp*BCG.

D. Phagosomes positive for colocalization are shown; data averaged from three separate experiments show increased *phox* colocalization for *gfp*Δ*fbpA* versus *gfp*D*BCG* and *gfpH 37Rv*.

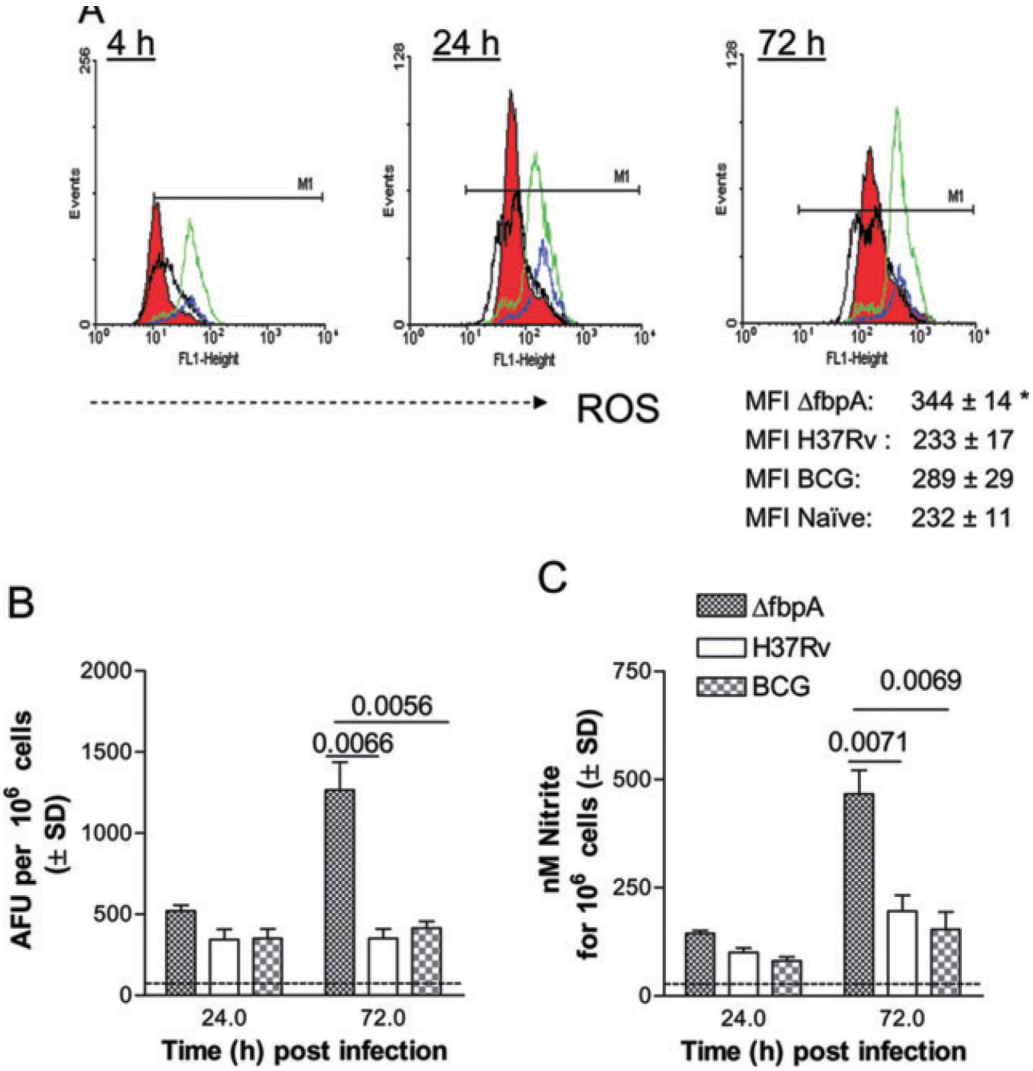

Fig. 5.

A. Intracellular oxidative activity within MΦs infected with Δ*fbpA,* BCG and H37Rv. MΦs or C57BL/6 bone marrow (BM)-derived BMA.A3 macrophage cell lines (both similar, MΦs shown) were infected with mycobacteria at an moi of 1:1, washed and incubated for 72 h. A. At time points shown, cells were treated with 1 μg ml^{-1} dihydrodichloro-fluorescein diacetate (H_2DCFDA), a probe for intracellular reactive oxygen species (ROS) for 5 min, washed and analysed in BD-Facscan using Cellquest software. Viable naïve MΦs have a basal level of fluorescence indicated by a red fill. MΦs infected with Δ*fbpA* show an enhanced and sustained fluorescence over time (green). MΦs infected with H37Rv show minimal ROS activity (black) while BCG infected MΦs show an intermediate level (blue). A positive control of phorbol myristyl acetate (an agonist for ROS) activated MΦs showed a burst of activity that declines rapidly within minutes (not shown). Mean fluorescent intensity (MFI, inset) values for Δ*fbpA* calculated from triplicate experiments (one histogram illustrated) was significant using Student's *t*-test (**P* < 0.0092).

B and C. Fluorometry and colorimetry for oxidant activity in MΦs. MΦs were infected as above. Twenty-four and 72 h post infection, the cultures from triplicate experiments were tested for ROS using H_2DCFDA and fluorometry (B) and nitrite, a product of NO synthesis by MΦs using the Greiss reagent and colorimetry (C). Δ*fbpA* induces accumulation of

higher levels of ROS and nitrite and *P*-values are shown for *gfpΔfbpA* versus *gfpΔBCG* and *gfpH 37Rv* (Student's *t*-test). Background fluorescence for ROS or nitrite in uninfected MΦs is shown as a dotted line in both B and C.

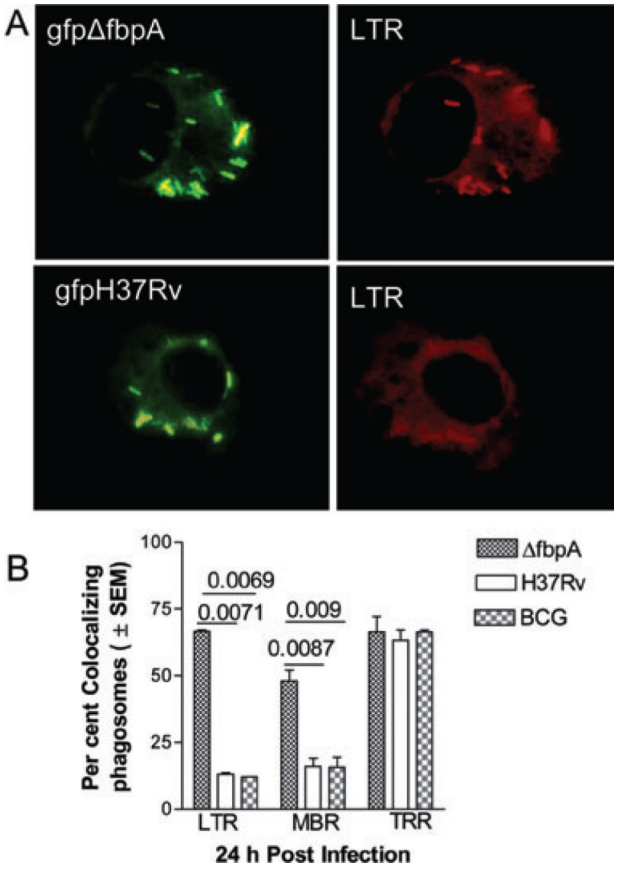

Fig. 6.

Δ*fbpA* phagosomes efficiently acquire both early and late endosomal markers when compared with H37Rv and BCG within MΦs. MΦs were labelled with lysotracker red (LTR), mannosylated BSA rhodamine (MBR), or transferrin Texas red (TRR), chased with medium and infected with *gfp*Δ*fbpA*, *gfp*BCG or *gfpH* 37Rv strains. MΦs were washed and examined for fluorescence colocalization.

A. LSM profile illustrates that live *gfp*Δ*fbpA* has markedly enhanced colocalization with LTR while the wild-type *gfpH* 37Rv excludes LTR.

B. Per cent phagosomes positive for colocalization was determined by using LSM in three separate experiments. *gfp*Δ*fbpA* significantly colocalizes with both LTR and MBR compared with either *gfp*BCG or *gfpH* 37Rv (Student's *t*-test). Colocalization with TRR, an early endosomal fusion marker, was comparable for all three strains tested. Scoring was carried out as in Fig. 4.

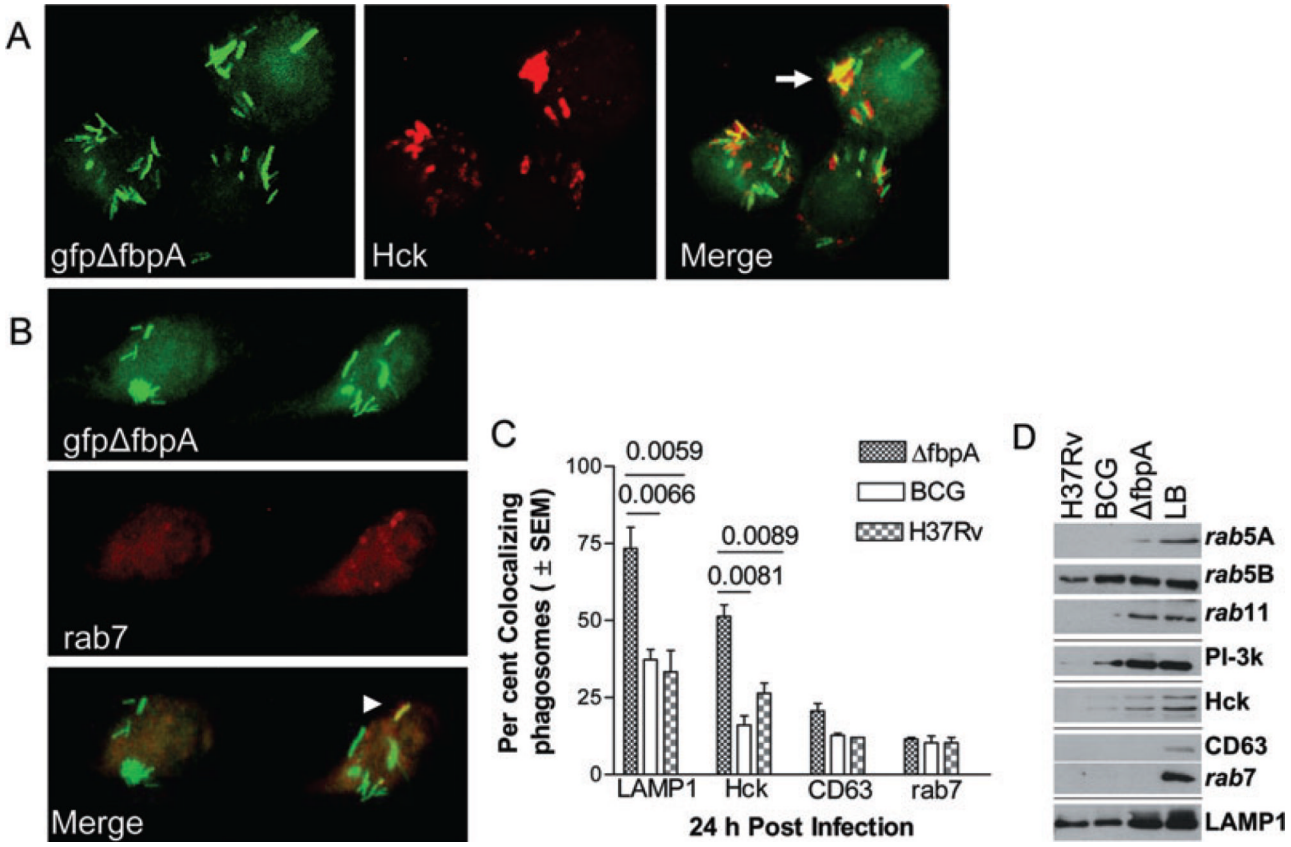

Fig. 7.

Δ*fbpA* phagosomes acquire late endosomal maturation markers but exclude lysosomal markers. MΦs were infected with *gfp*Δ*fbpA, gfpH*37Rv and *gfp*BCG strains for 4 h, washed and incubated for 24 h. MΦs were fixed, permeabilized and stained for three markers of late endosomes (lysosome-associated membrane protein 1, LAMP-1; *src* family kinase, Hck) and lysosomes (CD63 and *rab*7) using specific antibodies and counterstained with anti-Ig-Texas red conjugates. Phagosomes were examined for colocalization (arrow and arrowhead).

A. LSM profile illustrates that *gfp*Δ*fbpA* has an enhanced colocalization (arrow) with the Hck.

B. Illustration that *gfp*Δ*fbpA* largely excludes *rab*7.

C. Per cent phagosomes positive for fluorescence colocalization with the markers was determined by using LSM. *gfp*Δ*fbpA* phagosomes are more enriched for LAMP-1 and Hck but not CD63 and *rab*7. *gfp*BCG and *gfpH* 37Rv also acquire LAMP-1 to a lower level but exclude Hck, CD63 and *rab*7. Scoring from three separate experiments was averaged and significance determined using Student's *t*-test.

D. MΦs were infected with mycobacteria at an moi of 1:1 and phagosomes were purified on sucrose gradients at 24 h post infection. Latex beads (LB) were internalized for 4 h and phagosomes prepared as a positive control. Phagosomal proteins were then analysed using Western blot with specific antibodies followed by anti-Ig conjugates and HRP-dependent chemiluminescence. LB phagosomes acquire nearly all docking proteins along with CD63 and *rab7,* the specific marker of lysosomes. *gfp*Δ*fbpA* phagosomes acquire multiple markers that suggest an ability to fuse with early and recycling endosomes such as *rab5A, rab5B* and *rab11*. While they acquire late endosomal markers such as Hck, they exclude lysosome-specific markers like CD63 and *rab7*. LAMP-1 and phosphatidyl inositol-3-kinase

are also enriched on LB and *gfp*Δ*fbpA* phagosomes compared with *gfp*BCG and *gfpH* 37Rv.

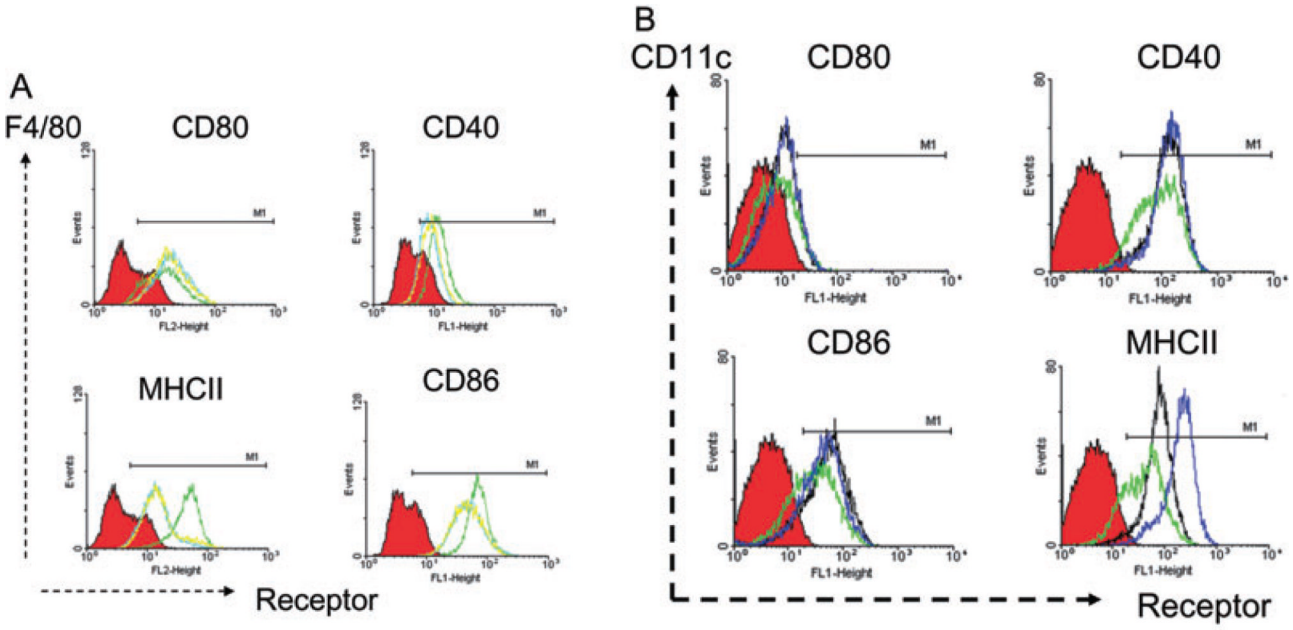

Receptor	Naive	ΔfbpA	BCG	H37Rv
CD40	79 ± 14	155 ± 22*	123 ± 21	108 ± 12
CD80	87 ± 15	108 ± 28	127 ± 21	123 ± 17
CD86	99 ± 15	187 ± 18**	129 ± 20	129 ± 18
MHC-II	89 ± 12	199 ± 16***	112 ± 23	119 ± 11
CD1d	144 ± 17	233 ± 44#	178± 16	155 ± 43

Receptor	Naive	ΔfbpA	BCG	H37Rv
CD40	66 ± 28	176± 27	189± 22	155 ± 12
CD80	78± 17	122 ± 14	119 ± 19	117 ± 14
CD86	77 ± 11	126 ± 14	131 ± 31	127 ± 22
MHC-II	89 ± 11	269 ± 21*	144 ± 11	107 ± 12
CD1d	121 ± 23	322 ± 18**	189 ± 34	119 ± 39

Fig. 8.

The Δ*fbpA* mutant induces an enhanced expression of MHC-II and CD1d molecules in MΦs and dendritic cells (DCs).

A. MΦs or BM-derived BMA.A3 cell line MΦs (both showed similar results, MΦs shown) were infected with mycobacteria at an moi of 1:1 for 4 h, washed, incubated for 24 h and stained for surface receptor expression using specific antibodies conjugated to fluorochromes. Receptor expression was analysed using BD-Facscan and Cellquest software. MΦ histograms (one of three experiments illustrated) show the unstained or isotype stained cells (red fill); Δ*fbpA* (green); H37Rv (blue) and BCG (yellow) infected MΦs. Histograms illustrate that MΦs infected with Δ*fbpA* show an enhanced expression of CD40, CD86 and MHC-II when compared with BCG- or H37Rv-infected MΦs. Mean fluorescence intensity values (MFIs) from triplicate separate experiments are shown below the histograms (*$P < 0.01$; **$P < 0.007$; ***$P < 0.008$; #0.01 compared with H37Rv- or BCG-infected MΦs, Student's *t*-test).

B. BM-derived CD11c bead purified DCs were infected and analysed for receptor expression as above. Histograms illustrate that Δ*fbpA* (blue) induces a stronger expression of MHC-II in DCs than BCG (black) or H37Rv (blue). MFIs from three independent

experiments are shown below the histograms (*$P < 0.009$; **$P < 0.009$ compared BCG- or H37Rv-infected DCs, Student's *t*-test).

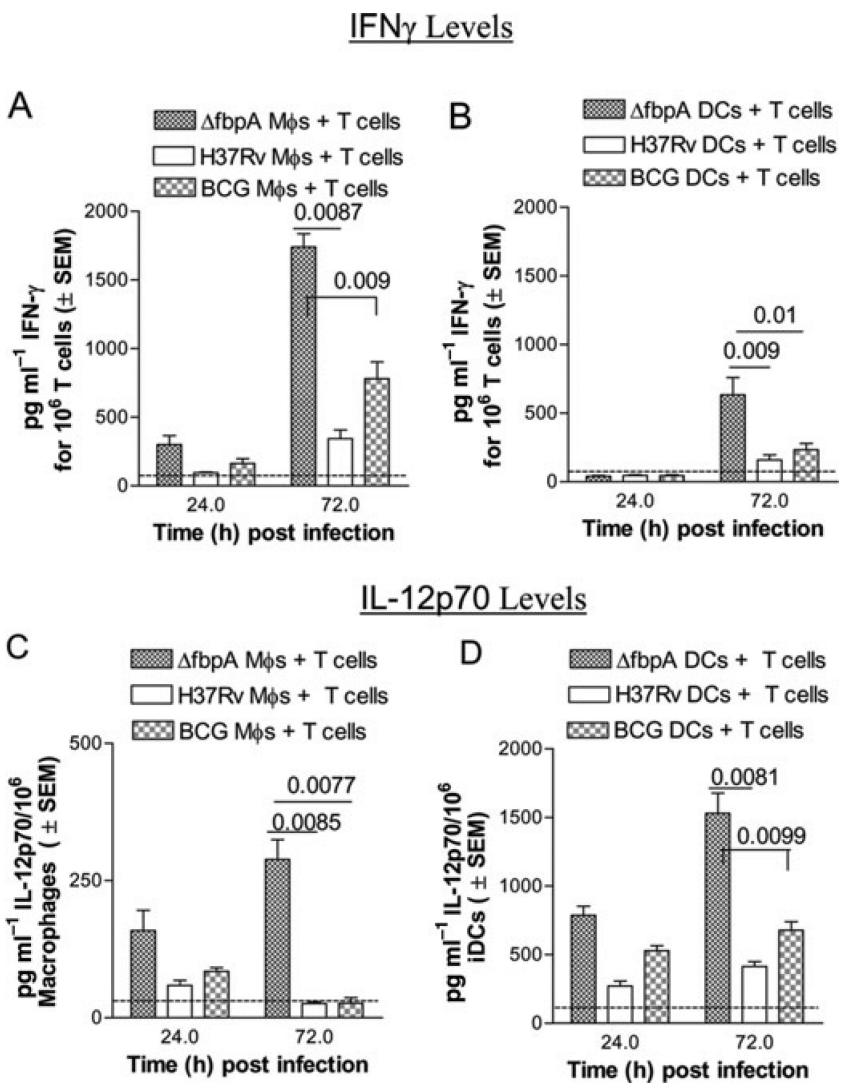

Fig. 9.

Δ*fbpA* is more immunogenic in MΦs or DCs than H37Rv or BCG. Antigen-presenting cells (APCS) such as MΦs (A, C) or DCs (B, D) were infected with mycobacteria for 4 h, washed and co-cultured with naïve or sensitized CD3-bead purified T cells from spleens of mice immunized with Mtb. After 72 h, the culture supernatants were assayed for IFN-γ (A and B) or IL-12p70 (C,D) using sandwich ELISA.

A and B. Δ*fbpA* induces a stronger response of IFN-γ in immune T cells (shown as bars) than BCG or H37Rv within MΦs (A) or DCs (B) (*P*-values determined using Student's *t*-test). Neither naïve T cells co-cultured with infected APCs nor uninfected APCs secrete significant levels of IFN-γ. The IFN-γ levels for these controls are represented as horizontal dotted lines.

C and D. Δ*fbpA* infected MΦs (C) or DCs (D) show elevated levels of IL-12p70 compared with BCG or H37Rv. Basal levels of IL-12p70 in uninfected in APCs or naïve T cell co-cultures are shown as horizontal dotted lines.